

# 1 Runaway breakdown and electrical discharges in thunderstorms

2 Gennady Milikh<sup>1</sup> and Robert Roussel-Dupré<sup>2</sup>

3 Received 22 August 2010; revised 2 August 2010; accepted 22 September 2010; published XX Month 2010.

4 [1] This review considers the precise role played by runaway breakdown (RB) in  
 5 the initiation and development of lightning discharges. RB remains a fundamental research  
 6 topic under intense investigation. The question of how lightning is initiated and  
 7 subsequently evolves in the thunderstorm environment rests in part on a fundamental  
 8 understanding of RB and cosmic rays and the potential coupling to thermal runaway  
 9 (as a seed to RB) and conventional breakdown (as a source of thermal runaways). In  
 10 this paper, we describe the basic mechanism of RB and the conditions required to initiate  
 11 an observable avalanche. Feedback processes that fundamentally enhance RB are  
 12 discussed, as are both conventional breakdown and thermal runaway. Observations  
 13 that provide clear evidence for the presence of energetic particles in thunderstorms/  
 14 lightning include  $\gamma$ -ray and X-ray flux intensifications over thunderstorms,  $\gamma$ -ray and  
 15 X-ray bursts in conjunction with stepped leaders, terrestrial  $\gamma$ -ray flashes, and neutron  
 16 production by lightning. Intense radio impulses termed narrow bipolar pulses  
 17 (or NBPs) provide indirect evidence for RB particularly when measured in association  
 18 with cosmic ray showers. Our present understanding of these phenomena and their  
 19 enduring enigmatic character are touched upon briefly.

20 **Citation:** Milikh, G., and R. Roussel-Dupré (2010), Runaway breakdown and electrical discharges in thunderstorms,  
 21 *J. Geophys. Res.*, 115, XXXXXX, doi:10.1029/2009JA014818.

## 22 1. Predecessors of Runaway Breakdown

23 [2] The many interesting things that happen when an  
 24 electric field is applied across a gas have occupied the  
 25 attention of physicists for more than a century since 1900  
 26 when Townsend discovered the laws governing ionization  
 27 and the gaseous discharge in a uniform electric field. These  
 28 studies have led to such fundamental discoveries as cathode  
 29 rays and X-rays, the fundamental properties of electrons and  
 30 atoms, and optical and mass spectrometry. Gas discharge  
 31 phenomena are now thought of as part of the field of plasma  
 32 physics [MacDonald, 1967; Brown, 1959; Gurevich *et al.*,  
 33 1997b].

34 [3] An avalanche breakdown in gases occurs when a large  
 35 electric field accelerates free electrons to energies high  
 36 enough to cause ionization during collisions with atoms.  
 37 The number of free electrons is thus increased rapidly as  
 38 newly generated particles become part of the process. The  
 39 conditions at which the gas “breaks down” or at which  
 40 sparking begins was naturally studied early and extensively,  
 41 and such studies have occupied a central place in gas dis-  
 42 charge phenomena over the years. However, a new type of  
 43 breakdown which plays an important role in thunderstorms  
 44 was discovered only recently [Gurevich *et al.*, 1992]. This  
 45 process is triggered by seed relativistic electrons that can

multiply rapidly in an applied electric field while at the same 46  
 time freeing large number of low-energy electrons, hence 47  
 the term runaway breakdown (RB), and it requires a break 48  
 even field an order of magnitude less than that needed to 49  
 initiate conventional breakdown. The purpose of this paper 50  
 is to describe the known properties of RB along with its 51  
 manifestation in the atmosphere. Before discussing the 52  
 physics of RB, we describe its predecessors, those studies 53  
 that ultimately led to the discovery of RB. 54

[4] Let us first discuss conventional air breakdown from 55  
 the standpoint of kinetic theory. When an electric field is 56  
 applied to air having some seed electrons their distribution 57  
 function changes from a Boltzmann distribution to that 58  
 having a plateau and high-energy tail as shown in Figure 1a. 59  
 These distributions are computed for different intensities of 60  
 the applied electric field. The higher the field intensity, the 61  
 smaller is the lower energy boundary of the tail. Electrons 62  
 with energy greater than the oxygen ionization threshold at 63  
 approximately 12.2 eV are involved in the avalanche break- 64  
 down. However, a competition exists between ionization and 65  
 dissociative attachment of electrons to molecular oxygen. The 66  
 cross sections of these processes are shown in Figure 1b. 67  
 Attachment has a relatively low cross section, although it 68  
 peaks at a low energy of 5.2 eV. The rates of ionization and 69  
 attachment equate at  $E = E_{th}$ , where  $E_{th} = 3$  MV/m is the 70  
 threshold field of air breakdown at standard temperature 71  
 and pressure (STP). 72

[5] Consider now what happens if the external electric field 73  
 significantly exceeds the breakdown threshold. As shown by 74  
 experiments in tokomaks [Sharma and Jayakumar, 1988] it 75

<sup>1</sup>University of Maryland, College Park, Maryland, USA.

<sup>2</sup>SciTech Solutions, LLC, Santa Fe, New Mexico, USA.

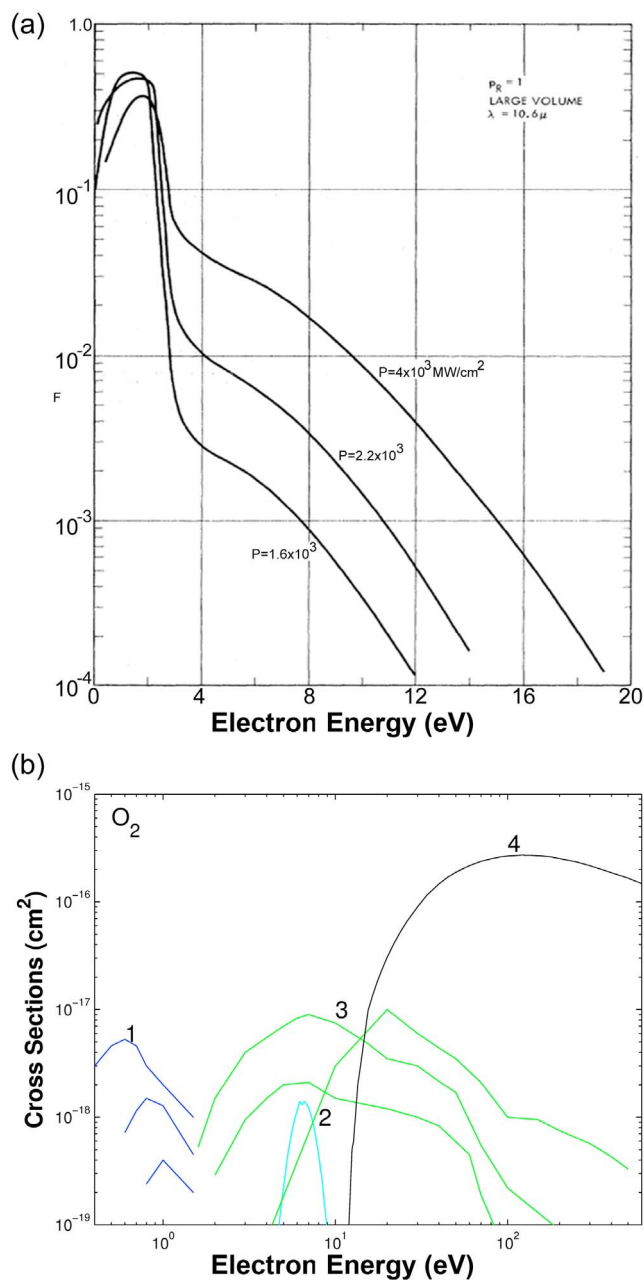


**Figure 1.** (a) The electron distribution functions in air computed for three different values of incident power density [adapted from *Kroll and Watson, 1972*]. (b) Cross-section for inelastic collisions of electrons with molecular oxygen [adapted from *Tsang et al., 1991*]: trace 1, the excitation of the vibrational levels, trace 2, dissociative attachment; trace 3, excitation of electronic levels; trace 4, the ionization cross section.

76 can lead to thermal runaway when the accelerated plasma hits  
77 the facility walls. The concept of electron runaway acceler-  
78 ation in the presence of a uniform, steady electric field was  
79 developed by *Gurevich* [1961], *Dreicer* [1960], and *Lebedev*  
80 [1965]. The runaway phenomenon is a consequence of the  
81 long range, small angle scattering among charged particles

undergoing Coulomb interactions. The scattering cross  
82 section decreases with velocity as  $\sigma_{tr} \sim 1/v^4$ . As a result, for  
83 a given electric field value the threshold energy can be  
84 found beyond which the dynamical friction cannot balance  
85 the acceleration force due to the electric field, resulting in  
86 continuous electron acceleration. 87

[6] In the weakly ionized plasma an important role is  
88 played by the electron-neutral collisions. Thus the cold  
89 electrons undergo the dynamical friction force, the latter  
90 playing a fundamental role in breakdown studies, 91

$$F = mv_{en} v, \quad (1)$$

where  $v_{en}$  is the electron-neutral collision frequency. The  
92 friction force is shown as the trace 1 in Figure 2 as a  
93 function of the electron kinetic energy, where it increases  
94 with  $\varepsilon$ . However, at high-electron velocity, when the  
95 electron energy exceeds the ionization potential ( $\varepsilon > \varepsilon_i$ ),  
96 the interactions of the fast electrons with the nuclei and  
97 atomic electrons obey the Coulomb law. Correspondingly  
98 the dynamical friction force decreases with the electron  
99 energy [*Bethe and Ashkin, 1953*], 100

$$F = m\nu(v)v = \frac{4\pi e^4 n}{mv^2} \ln \Lambda, \quad (2)$$

where  $n$  is the electron density and  $\ln \Lambda$  is the Coulomb  
101 logarithm. This force is shown as trace 2 in Figure 2. 102  
*Gurevich* [1961] first introduced the critical electric field  
103 for thermal runaway. Its value is 104

$$E_{cn} = \frac{4\pi e^3 Z N_m k_n}{\varepsilon_i}, \quad (3)$$

here  $N_m$  is the density of the neutral molecules and  $Z$  is the  
105 mean molecular charge, which for air is 14.5, and  $k_n$  is the  
106 numerical factor, determined by the type of the neutral gas. 107  
In fact, for hydrogen,  $k_n \sim 0.33$ , and for helium,  $k_n \sim 0.30$ . 108

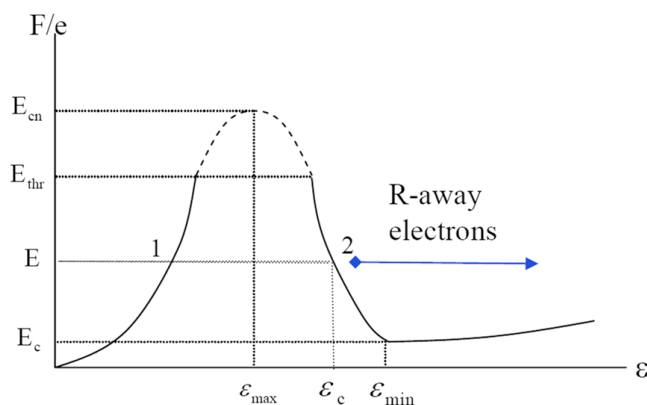


**Figure 2.** Schematic of the dynamical friction force in air as a function of electron energy. Traces 1 and 2 correspond to low- and high-energy electrons, respectively.  $E_{cn}$  is the critical field for thermal runaway,  $E_{thr}$  is the breakdown threshold, and  $E_c$  is the critical field for relativistic breakdown.

109 [7] If the electric field is larger than  $E_{cn}$ , the entire  
110 population of electrons is accelerated and gains energy. If  
111 the field is less than  $E_{cn}$ , only a few electrons having  
112 energy higher than  $\varepsilon_c$  are accelerated,

$$\varepsilon > \varepsilon_c = \frac{2\pi e^3 Z N_m \ln \Lambda_n}{E}, \quad (4)$$

113 where  $\Lambda_n \sim \varepsilon_c / Z \varepsilon_i$ . These are the runaway electrons in the  
114 neutral gas, and according to *Gurevich* [1961], their flux is  
115 given by

$$S_r = n\nu_e \exp\left\{-\frac{E_{cn}}{4E}A\right\}, \quad (A = 30 \text{ for air}). \quad (5)$$

116 We emphasize that the amplitude of the electric field  
117 leading to the electron runaway is limited, since only for  
118 nonrelativistic electrons does the dynamical friction force  
119 drop when the electron energy increases [*Bethe and Ashkin*,  
120 1953]. For relativistic electrons the friction force reaches its  
121 minimum at the energy  $\varepsilon_m \sim 1.4$  MeV and then slowly  
122 (logarithmically) increases with  $\varepsilon$  (see Figure 2). The  
123 minimum of the friction force  $F_{\min}$  is related to the mini-  
124 mum value of the electric field  $E_c$ , which still generates the  
125 runaway, this field is called critical field, and its value is

$$E_c = \frac{4\pi Z e^3 N_m}{mc^2} a \quad (6)$$

126 in the air,  $a \sim 11.2$ . Notice that the following relations hold

$$\frac{E_{cn}}{E_c} \approx \frac{mc^2}{30\varepsilon_i} \approx 200, E_{cn} \approx 10E_{th}, E_c \approx E_{th}/20. \quad (7)$$

127 Therefore, in the air, the runaway electrons could appear in  
128 a wide range of electric field  $E_c < E < E_{cn}$ , which spans  
129 almost 3 orders of magnitude.

130 [8] This basic kinetic description of electron acceleration,  
131 energy loss, and ionization that occurs throughout the  
132 energy range from zero to tens of MeV forms the basis for  
133 understanding electrical breakdown in gases and various  
134 materials. The specifics of the electron-neutral interactions  
135 that govern electron transport at high energy ( $>1-10$  keV)  
136 and the associated production of secondary electrons allow  
137 for quantification of the RB mechanism. Details are pro-  
138 vided below along with a historical overview of advances  
139 made in understanding the role of RB in thunderstorm  
140 electrical processes.

## 141 2. Basic Mechanism and Advances in 142 Understanding of Runaway Breakdown

143 [9] The basic mechanism by which relativistic electrons  
144 avalanche and break down dielectrics such as neutral gases  
145 was first described by *Gurevich et al.* [1992]. Preceding this  
146 work were the measurements of enhanced X-ray fluxes in  
147 thunderstorms and the corresponding theoretical analyses by  
148 *McCarthy and Parks* [1992] that clearly pointed to a need  
149 for multiplication of the energetic electrons to account for  
150 the high measured fluxes of bremsstrahlung photons. In  
151 addition to acceleration and runaway in thunderstorm  
152 electric fields *Wilson* [1924] also hinted at potential multi-  
153 plication of the energetic electrons by secondary ionization,

154 however, the details of this process and its implications  
155 for lightning discharges were not worked out until 1992  
156 (see paper by *Williams* [2010]).

157 [10] As noted in the previous section the quantitative  
158 studies of runaway acceleration by both *Dreicer* [1960] and  
159 *Gurevich* [1961] in the context of fusion plasmas also  
160 helped to set the stage for the development of the RB  
161 mechanism. Using the insight provided in these works and  
162 in the 1992 paper, the detailed kinetic theory of RB was  
163 formulated by *Roussel-Dupré et al.* [1994] and subsequent  
164 work that significantly improved and refined the computed  
165 avalanche rates [*Symbalisky et al.*, 1998; *Lehtinen et al.*,  
166 1999; *Gurevich and Zybin*, 2001; *Babich et al.*, 1998,  
167 2001a] in basic agreement with the initial estimates obtained  
168 in 1992. A recent more detailed review and extended  
169 analysis at low electron energies is provided in *Roussel-  
170 Dupré et al.* [2008].

171 [11] One of the important quantitative aspects of RB is the  
172 steady-state rate at which the energetic population of elec-  
173 trons multiplies for different applied electric field strengths.  
174 A plot of the avalanche times ( $\tau$ ) (sometimes referred to as  
175 “the characteristic e-folding time”) as a function of the  
176 overvoltage  $\delta_0 = E/E_c$  for air at STP as computed by  
177 *Roussel-Dupré et al.* [2008] is reproduced in Figure 3a  
178 along with the corresponding mean energy  $\varepsilon_m$ , Figure 3b,  
179 and the energy spread about the mean  $\varepsilon_{\text{sig}}$ , Figure 3c, of the  
180 electron population. A general form that yields agreement to  
181 within 2% throughout the range  $1.5 < \delta_0 < 25$  for each of  
182 these quantities can be written,

$$Y = \frac{A}{(\delta_0 - 1.28)^B} \exp\left[C \ln(\delta_0 - 1.28)^2 + D \ln(\delta_0 - 1.28)^3 + E \ln(\delta_0 - 1.28)^4\right], \quad (8)$$

183 where  $Y$  represents either  $\tau$ ,  $\varepsilon_m$ , or  $\varepsilon_{\text{sig}}$  and  $A-E$  are the  
184 corresponding fit parameters determined by a polynomial  
185 least squares fitting routine. The fit parameters are provided  
186 in Table 1.

187 [12] The results for  $\delta_0 > 10$  do not include contributions  
188 that may come from the conventional avalanche of low-  
189 energy ( $<100$  eV) electrons. The coupling that exists  
190 between the low-energy electrons and the relativistic  
191 runaway electrons for applied fields that exceed the  
192 conventional breakdown threshold is discussed below in  
193 more detail [cf., *Colman et al.*, 2010]. Note that the  
194 mean energy of the electrons can exceed 7 MeV with a  
195 spread greater than 12 MeV. The electron distribution  
196 function is shown in Figure 4 for an over-voltage of  $\delta_0 = 4$   
197 as a function of electron energy  $\varepsilon$  and the angle  $\theta$  of  
198 motion of the electrons relative to the direction of the  
199 electric field. Note the collimation of the electrons along  
200 the electric field at high energies. These electrons consti-  
201 tute a particle beam propagating antiparallel to the electric  
202 field. The steady state form of the distribution function is  
203 achieved when the rate at which particles accelerate to  
204 higher energies  $R = ec(E-E_c)/\varepsilon_m$  is equal to the avalanche  
205 rate,  $R_a = 1/\tau$ . From this equality one obtains a simple  
206 expression for the mean energy of the electrons in terms  
207 of the avalanche time,  $\varepsilon_m = ce(E-E_c)\tau = ceE_c(\delta_0-1)\tau$ .  
208 In units of eV this expression becomes  $\varepsilon_m = 2.2 \times 10^5$   
209  $(\delta_0-1)l_{av}$ , where  $l_{av}$  is the avalanche length (taken to be  $c\tau$ )

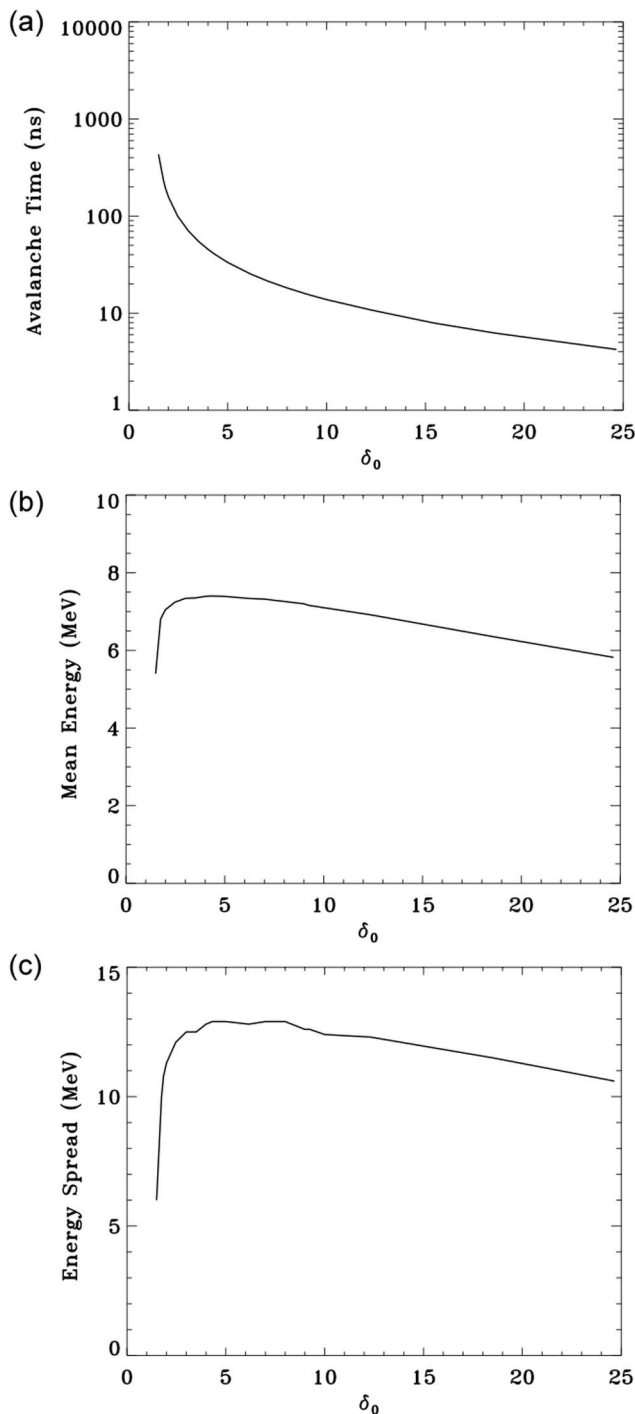


**Figure 3.** (a) Avalanche time in ns. (b) Mean electron energy in MeV. (c) Electron energy spread in MeV as a function of the over-voltage  $\delta_0 = E/E_c$ . All calculations were performed for air at STP.

210 in meters. A check of this result against equation (8) confirms  
211 the basic physical assumption for a steady state solution.

212 [13] At this stage in the development of the RB mecha-  
213 nism, the details of the electron distribution function were  
214 understood for the case of a steady, uniform, externally  
215 applied electric field. The basic properties of RB in this case  
216 include a threshold field ( $\sim 280$  kV/m at STP) for initiation

of an avalanche that is approximately a factor of 10 less than  
conventional breakdown, high mean energies  $\sim 7$  MeV,  
bremsstrahlung radiation to 20 MeV and possibly higher,  
and spatial avalanche scales from 2 to 70 m at STP. Sub-  
sequently our theoretical understanding of RB was advanced  
through studies of the spatial evolution of a runaway dis-  
charge including the effects of diffusion [Gurevich *et al.*,  
1994], calculations of the X-ray emissions produced by  
RB in thunderstorms [Gurevich *et al.*, 1997a], and appli-  
cations of RB to the development of discharges driven by  
the thunderstorm electric field. The latter included models  
for sprites [Taranenکو and Roussel-Dupre, 1996; Roussel-  
Dupr e and Gurevich, 1996, Yuxhimuk *et al.*, 1999], blue  
jets [Yuxhimuk *et al.*, 1998], and intracloud discharges  
[Roussel-Dupr e *et al.*, 2003]. We note that the mechanism  
of RB encompasses both an avalanche of relativistic elec-  
trons and the copious production of low-energy secondary  
electrons that contribute significantly to the total electrical  
current and play an essential role in the evolution of an RB  
discharge [cf., Gurevich *et al.*, 2004b].

[14] The application of RB to the modeling of high-altitude  
discharges necessitated a more detailed analysis of the effect  
of an externally applied magnetic field on the kinetics of the  
runaway process and the corresponding avalanche rates  
[Gurevich *et al.*, 1996; Lehtinen *et al.*, 1999]. Depending on  
the angle relative to the electric field, the magnetic field  
suppresses RB as the electrons become magnetized and are  
accelerated by only a fraction of the total electric field  
strength. These effects become important in the atmosphere  
above approximately 20 km altitude where MeV electrons  
become magnetized.

[15] In 1999 Gurevich *et al.* suggested that cosmic rays  
and extensive air showers could play an important role in  
providing the seed energetic electrons needed to initiate a  
strong RB discharge. The number of seed electrons per unit  
area increases with the energy of the primary cosmic ray  
particle as

$$\rho_e = 0.4 \frac{n_0}{R^2} \left(\frac{R}{r}\right)^2 \left(1 + \frac{r}{R}\right)^{-3.5} \text{ with } n_0 = 0.3 \frac{\varepsilon_{cr}}{\beta \sqrt{\ln(\varepsilon_{cr}/\beta)}},$$

where we have taken  $s = 1$  in equation (2) of Gurevich *et al.*  
[1999a],  $R \sim 115$  m in air,  $\varepsilon_{cr}$  is the incident cosmic ray  
particle energy,  $r$  is the distance from the shower axis, and  
 $\beta = 72$  MeV for air. The frequency of these showers is given  
by  $5 \times 10^3 (10^{13}/\varepsilon_{cr})^2 \text{ km}^{-2} \text{ sr}^{-1} \text{ s}^{-1}$  and the minimum  
energy to initiate RB was estimated to be  $\sim 10^{15}$  eV. The  
frequency of EAS at these energies fits well with the mea-  
sured rate of intracloud lightning for typical charge layer  
dimensions. In addition, the production of radio frequency  
(RF) radiation by an RB discharge was analyzed and found  
to possess a characteristic bipolar temporal signature [cf.,  
Roussel-Dupr e and Gurevich, 1996; Gurevich *et al.*, 2003].  
This fact was exploited by Gurevich *et al.* [2004a] to look  
for a correlation between cosmic ray showers and the initia-  
tion of intracloud lightning.

[16] The large scale lengths associated with RB in gases  
make it difficult to reproduce in the laboratory. Two experi-  
ments [Gurevich *et al.*, 1999b; Babich *et al.*, 2004a] have  
been conducted with some success but interpretation of the  
results requires careful analysis of the experimental setup and  
associated diagnostics. A more straightforward experimental

t1.1 **Table 1.** Fit Parameters for  $\tau$ ,  $\varepsilon_m$ , or  $\varepsilon_{sig}$  With Results in ns, MeV, and MeV, Respectively

	A	B	C	D	E	
t1.2	$\tau$	117.154	0.90331769	-0.028990976	-0.0054570445	0
t1.3	$\varepsilon_m$	7.2369	-0.047166287	-0.044739548	0.023395940	-0.0066729225
t1.4	$\varepsilon_{sig}$	12.0186	-0.13104670	-0.11326119	0.051383081	-0.010414670

275 configuration with larger scale lengths is needed in order to  
 276 systematically study the RB mechanism under controlled  
 277 conditions that yield reliable/repeatable results. Acquiring an  
 278 appropriate facility may well require some technological  
 279 breakthroughs so, for now, we are left with the natural  
 280 environment to provide us with validation and further details  
 281 regarding RB.

282 [17] In 2003, Dwyer pointed to the important role played  
 283 by secondary emissions ( $\gamma$ -rays and positrons) in enhancing  
 284 the RB process by providing additional seed energetic  
 285 electrons in the source region in the same way that photon  
 286 and ion feedback mechanisms at the cathode work in con-  
 287 ventional breakdown experiments conducted in the labora-  
 288 tory [e.g., *Morrow*, 1985a, 1985b; see also *Dwyer*, 2008].

289 [18] To better understand how the RB mechanism oper-  
 290 ates in air and appreciate the overlap that exists among the  
 291 processes of RB, thermal runaway, and conventional  
 292 breakdown we refer the reader to a companion paper pub-  
 293 lished in this special issue [*Colman et al.*, 2010]. Figure 5  
 294 shows a more detailed plot of the energy loss rate for  
 295 electrons in air with the vibrational transitions of Oxygen  
 296 and Nitrogen included. For an applied field above the high-  
 297 energy minimum at  $\varepsilon_m \sim 1.4$  MeV and below the maximum  
 298 at  $\varepsilon_p \sim 100$  eV, it is possible to divide the energy space into  
 299 two regimes we shall call thermal, where  $\varepsilon < \varepsilon_1$ , and run-  
 300 away, where  $\varepsilon > \varepsilon_2$ .  $\varepsilon_1$  is the energy below  $\varepsilon_p$  at which the  
 301 electric field equals the energy loss rate and similarly for  $\varepsilon_2$

302 which lies above  $\varepsilon_p$ . These two kinetic regions interact with  
 303 each other by means of two mechanisms. Thermal electrons  
 304 can leak into the runaway regime by tunneling through the  
 305 intermediate energy region between  $\varepsilon_1$  and  $\varepsilon_2$  and runaway  
 306 electrons produce thermal electrons by direct ionization.  
 307 These two populations of electron feed back on each other  
 308 such that one or the other controls the growth rate of both  
 309 populations. When the applied field is below the threshold  
 310 for avalanche of the thermal population, the runaway elec-  
 311 trons define the rate of growth of both populations. When  
 312 the applied field is above the threshold for conventional  
 313 breakdown and the avalanche rate of the thermal electrons  
 314 exceeds the runaway avalanche rate then the thermal elec-  
 315 trons will ultimately define the growth rate of both popu-  
 316 lations. There is a time delay however before the thermal  
 317 population can leak sufficiently into the runaway regime to  
 318 dominate the runaway population. A quantitative treatment  
 319 of this kinetic interaction is provided by *Colman et al.*  
 320 [2010]. As noted previously, both Dreicer and Gurevich  
 321 addressed the thermal runaway process while *Moss et al.*  
 322 [2006] and *Gurevich et al.* [2007] described and referred to  
 323 a strong runaway breakdown regime where the electric field  
 324 exceeds the threshold for conventional breakdown ( $E > E_c$ )  
 325 and placed his results in the context of lightning stepped  
 326 leader development.

[19] In conclusion to this section we briefly summarize the  
 327 main features of Runaway Breakdown (RB). It is triggered  
 328

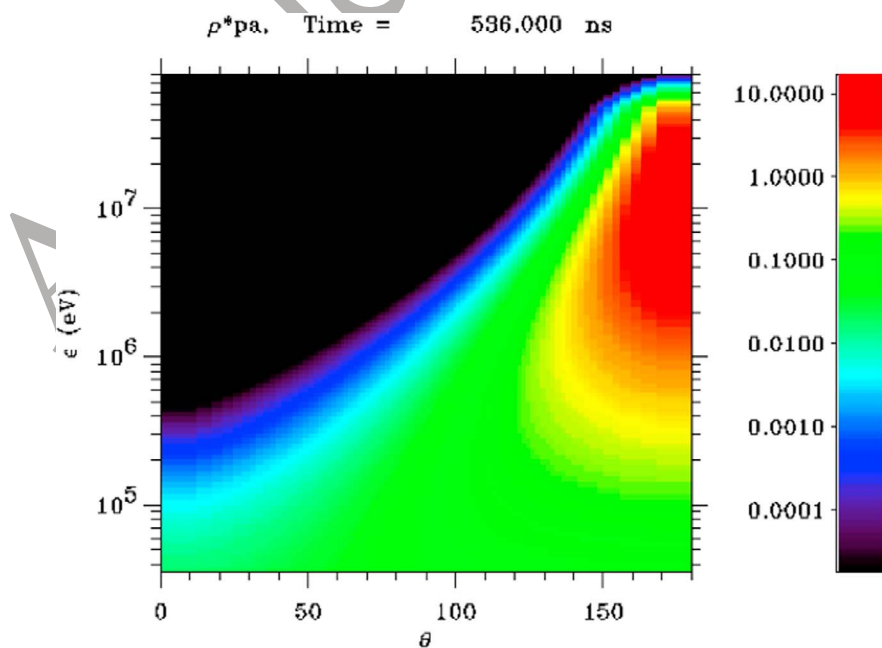


**Figure 4.** Electron distribution function for  $\delta_0 = 4$  as a function of electron energy  $\varepsilon$  in eV and the angle  $\theta$  of motion of the electrons relative to the direction of the electric field.

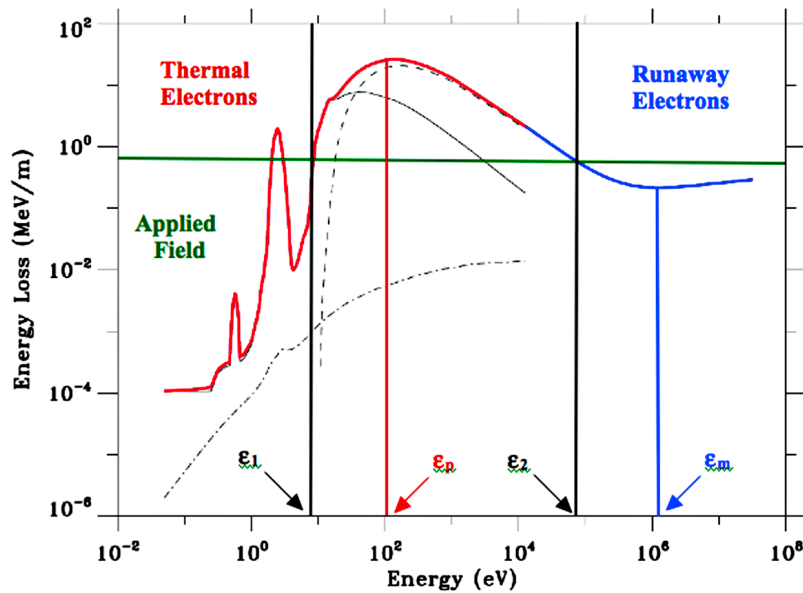


**Figure 5.** Energy loss rate for electrons in air as a function of electron energy. The red curve is derived from detailed cross sections for elastic, rotational, vibrational, electronic, and ionizing electron-neutral collisions in air. The solid, dashed, and dash-dotted curves represent the energy loss rate due to inelastic (sum of rotational, vibrational, and electronic processes), ionizing, and elastic collisions, respectively. The blue curve is the Bethe energy loss formula invoked at energies above 10 keV. The green line represents the magnitude of an applied electric field.  $\varepsilon_1$ ,  $\varepsilon_2$ ,  $\varepsilon_p$ , and  $\varepsilon_m$  are defined in the text.

329 by seed relativistic electrons and needs a break even field an  
 330 order of magnitude less than the conventional breakdown  
 331 threshold. The exponential growth of RB is determined by  
 332 the electrons in 3–200 keV energy range, although the high-  
 333 energy “tail” extends up to tens of MeV. This tail determines  
 334 the  $\gamma$ - and X-ray fluxes. The main population of electrons  
 335 generated by RB has low energy (1–3 eV) and these elec-  
 336 trons produce the electric current, electric field attenuation  
 337 and radio emission. Finally, unlike the conventional break-  
 338 down, our present understanding suggests that RB does not  
 339 happen in alternating or stochastic electric fields.

### 340 3. Manifestation of Runaway Breakdown 341 in the Atmosphere

342 [20] As mentioned in section 3, until recently laboratory  
 343 studies of RB have not yielded definitive results. A new  
 344 perspective is related to laboratory experiments based on  
 345 long sparks in air. They successfully detected X-ray bursts  
 346 having a broad energy spectrum up to a few MeV which are  
 347 presumably caused by RB [Dwyer *et al.*, 2005; Rahman  
 348 *et al.*, 2008]. The reported breakdown field was about  
 349 1.1 MV/m which is less than that of the conventional  
 350 breakdown although still much higher than that of RB  
 351 thus leaving some uncertainty about its RB nature. However  
 352 in the RB studies one can still mostly rely on the natural  
 353 phenomena that occur in thunderstorms and manifest  
 354 themselves by generating X-ray and  $\gamma$ -ray emissions, as  
 355 well as neutrons. The observations of emissions generated  
 356 by RB in thunderstorms will be reviewed in this section.

357 [21] Earlier attempts to detect X-rays due to thunderstorm  
 358 activity were focused on that caused by a strong current due

to the return stroke [d’Angelo, 1987; Hill, 1963]. Those 359  
 attempts were unsuccessful since the electron temperature in 360  
 the lightning channel does not exceed a few thousand K. 361  
 Thus the hot, thermal component of the lightning channel is 362  
 not a suitable source for X-ray production. 363

#### 364 3.1. Intracloud X-ray Pulses

[22] A breakthrough occurred when McCarthy and Parks 365  
 [1985, 1992] conducted observations while flying an aircraft 366  
 through thunderclouds with onboard X-ray detectors. It 367  
 was reported that (1) X-ray fluxes increased by 1–3 orders 368  
 of magnitude in all energy channels available (from 5 keV up to 369  
 110 keV), (2) the horizontal scale of the radiating region can 370  
 exceed several hundred meters, and (3) the elevated X-ray 371  
 production precedes a lightning flash by a few seconds and 372  
 ceases immediately after a lightning flash. 373

[23] The last finding was of special importance. It showed 374  
 that an, as yet, unknown mechanism of X-ray production 375  
 existed, which was not related to lightning flashes. Further- 376  
 more, McCarthy and Parks correctly attributed the observed 377  
 X-ray fluxes to bremsstrahlung by high-energy electrons. 378  
 They also assumed that the observed X-rays could be caused 379  
 by cosmic ray secondary electrons accelerated by the thun- 380  
 derstorm electric field. However, the number density of 381  
 energetic electrons available from cosmic ray secondaries is 382  
 more than an order of magnitude less than that required to 383  
 produce the observed X-ray fluxes. A magnification mech- 384  
 anism was missing, which role is played by runaway 385  
 breakdown. 386

[24] These experiments attracted interest to the direct X- 387  
 ray measurements in thunderclouds. Eack [1996] was the 388  
 first to fly a meteorological balloon equipped with a spe- 389

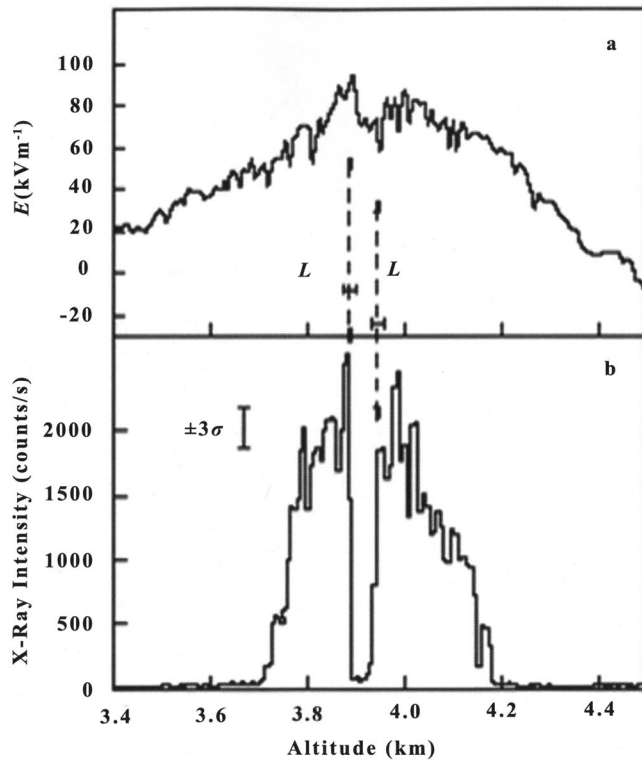


**Figure 6.** Balloon measurements of (top)  $E$  field and (bottom) X-rays [adapted from *Eack, 1996*].

390 cially designed light X-ray detector into a large thunder-  
391 storm [see also, *Eack et al. 1996*]. The balloon also carried  
392 an electric field meter.

393 [25] It was found that on a number of occasions the X-ray  
394 flux strongly increases for about 1 min in all three energy  
395 channels (30–120 keV) available. This is illustrated in  
396 Figure 6 which shows vertical profiles of X-ray intensity and  
397 electric field strength. A significant increase in X-ray counts  
398 near 4 km height is revealed and lasted for about 4 min.  
399 Simultaneously the electric field strength increased as well.  
400 In Figure 6, two arrows marked by letters L show lightning  
401 flashes, which precede significant decreases in the X-ray  
402 flux. Note also that *Marshall et al. [1995]* used balloons to  
403 measure the strength of thunderstorm electric field. Figure 7  
404 shows the results of the field measurements made along the  
405 balloon orbit as well as the curves which show the height  
406 profile of the critical field of the runaway breakdown. It is  
407 seen that the electric field can reach the RB threshold  $E_c$ .  
408 Here the arrows show that when the field reaches  $E_c$  it cor-  
409 relates with a lightning flash. *Marshall et al. [1995]* con-  
410 cluded from analysis of a number of thunderstorm electric  
411 field soundings that lightning may occur whenever the  
412 electric field exceeds the  $E_c$  value. Thus lightning may limit  
413 the electric field inside thundercloud to values less than  $E_c$ ,  
414 which indicates that RB could be a trigger mechanism for  
415 lightning. As suggested by *Gurevich and Milikh [1999]* RB  
416 leads to the charge transfer, by both ion and electron, which  
417 in turn reduces the thundercloud electric charge, and thus  
418 leads to redistribution of the electric field producing a  
419 characteristic flat-type electric field maximum observed  
420 earlier in thunderclouds [*Marshall et al., 1995*].

[26] These observations reveal that RB could occur inside 421  
thunderclouds at a few kilometers in height. To study such an 422  
effect one can either fly detectors through a thundercloud or 423  
just install them high up in the mountains and wait till a 424  
thunderstorm occurs. In fact, we discuss next three different 425  
observations of RB obtained in the mountains. The first one 426  
was conducted by the carpet air shower array at Baksan, 427  
North Caucasus at 1.7 km altitude during a thunderstorm on 428  
9 July 2000 [*Alexeenko et al., 2002*]. Shown in Figure 8 (top) 429  
are the electric field strength and so-called soft component of 430  
cosmic rays which describes electrons in the energy range 431  
10–30 MeV. Figure 8 reveals that a noticeable ( $\leq 20\%$ ) 432  
enhancement of the soft component of cosmic rays lasted 433  
about 0.5 min before the lightning flash and coincides with 434  
the flash. At the same time the hard component with energies 435  
exceeding 70 MeV (third plate from the top) was not 436  
affected. Finally, Figure 8 (bottom) shows an increase of the 437  
electric current due to thermal electrons generated by the RB. 438  
Notice that a peculiarity of RB is that the production of 439  
relativistic particles is accompanied by the production of 440  
thermal electrons having a velocity about 2 orders of mag- 441  
nitude less than that of relativistic electrons. However, since 442  
the total number of thermal electrons is 5–6 orders of mag- 443  
nitude higher than that of relativistic electrons the electric 444  
current is predominantly determined by thermal electrons. 445

[27] The second experiment also conducted inside a 446  
thunderstorm at a mountain observatory located 2.7 km 447  
above sea level provides proof of the existence of RB. 448  
During this experiment *Tsuchiya et al. [2009]* detected 449  
simultaneous bursts of runaway electrons and  $\gamma$ -rays which 450  
preceded lightning flashes. 451

[28] The last and the most sophisticated experiments 452  
among those reviewed here were conducted by Gurevich 453  
and his team during 2002–2009 at the Tien-Shang Mountain 454  
at 3.4–4 km above sea level [*Gurevich et al., 2009*]. They 455

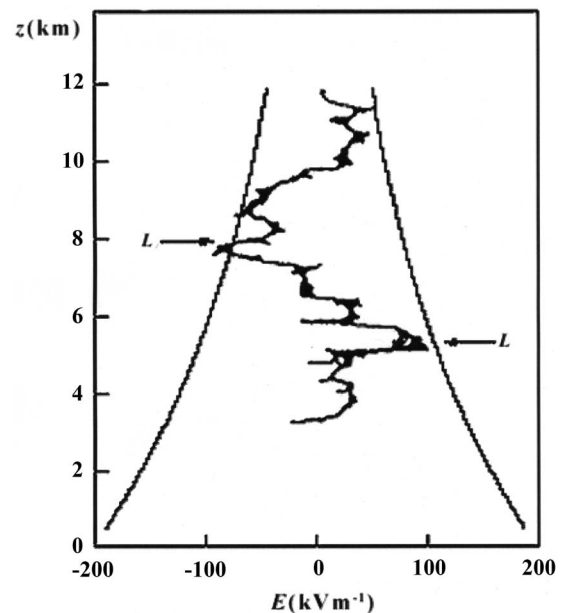


**Figure 7.** Balloon measurements of the electric field [adapted from *Marshall et al., 1995*]. The arrows marked L shows lightning strokes.

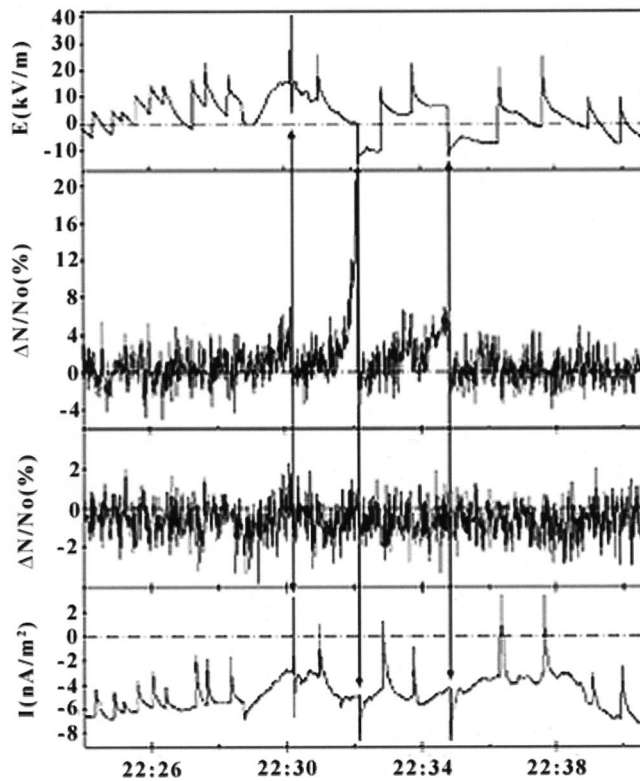


**Figure 8.** Observations by the Carpet air shower array at Baksan, North Caucasus during the thunderstorm on 9 July 2000. (top plate) The electric field and (second from the top) the soft component (electrons, 10–30 MeV) of cosmic rays. The arrows show lightning strokes [adapted from *Alexeenko et al.*, 2002].

456 looked for RB triggered by electron secondaries produced  
 457 by Extensive Atmospheric Showers (EAS) (see Figure 9).  
 458 Thus, they used an array of Geiger-Muller counters which  
 459 detect  $\gamma$ -rays caused by particles with energy in the range of  
 460  $2 \times 10^{14}$ – $10^{15}$  eV. A signal from the EAS triggered the radio  
 461 receiver which detects a radio pulse caused by currents of  
 462 both relativistic runaway electrons and thermal electrons  
 463 which is produced by the RB.

464 [29] As a result hundreds of simultaneous  $\gamma$  and radio  
 465 pulses were detected during thunderstorms. In the absence  
 466 of thunderstorms no radio pulses were observed although  
 467 EASs were always seen.

468 [30] The observed radio pulses were bipolar widths  
 469 ranging from 0.4 to 0.7  $\mu$ s. As we discuss later on in this  
 470 section, this time scale corresponds well to RB development  
 471 and duration at typical charge layer heights. Besides, the  
 472 intensity of the radio pulses due to RB corresponds to an  
 473 external electric field  $E = (1.2 - 1.4)E_c$ .

474 [31] A model of the X-rays due to RB inside thunder-  
 475 clouds was developed by *Gurevich et al.* [1997a]. The  
 476 model first estimates the total flux of ambient cosmic ray  
 477 secondary electrons. Then it computes the magnification of  
 478 this flux due to RB and finally finds the spectral density of  
 479 the bremsstrahlung emission. The latter is shown in  
 480 Figure 10 computed for the height 4 km at an electric field  
 481 twice the value of the critical field for RB. *Gurevich and*  
 482 *Milikh* [1999] studied X-ray propagation in the atmosphere

by taking into account Compton scattering and loss due to 483  
 photo ionization. The computed energy spectrum was then 484  
 checked against the spectrum observed by *Eack* [1996]. He 485  
 observed an X-ray event of 1 min duration, i.e., much longer 486  
 than any lightning flash. It is shown in Figure 11 where the 487  
 model X-ray fluxes were integrated over three energy 488  
 channels (30–60, 60–90, and 90–120 keV). The red points in 489  
 Figure 11 show the balloon measurements, the blue points 490  
 show the model spectrum at 70 m from the source, and the 491  
 green points show the model at 420 m from the source. The 492  
 latter case is in a good agreement with the observations. 493

### 3.2. Terrestrial $\gamma$ -ray Flashes

[32] The Earth's atmosphere becomes transparent to  $\gamma$ - 495  
 rays with energies greater than  $\sim 1$  MeV above about 25 km 496  
 altitude. As a result, strong  $\gamma$ -ray bursts originating at high 497  
 tropospheric altitudes and perhaps somewhat below the 498  
 tropopause can be seen from space-based platforms and can 499  
 in turn provide some diagnostic information about the 500  
 source. Indeed, TGFs were first discovered by the Burst and 501  
 Transient Source Experiment (BATSE) on the Compton  $\gamma$ - 502  
 ray Observatory (CGRO) [*Fishman et al.*, 1994] and are 503  
 presently being monitored by the Reuven Ramaty High 504  
 Energy Solar Spectroscopic Imager (RHESSI) satellite, 505  
 which has observed some 10–20 TGFs per month [*Smith*, 506  
*et al.*, 2005]. The Fermi  $\gamma$ -ray Space Telescope has also 507  
 recently detected TGFs [see *Fishman et al.*, 1994]. The 508  
 BATSE experiment consisted of eight large area detectors 509  
 (2000 cm<sup>2</sup> each, NaI crystals) situated on the corners of the 510  
 CGRO. The large number of counts (>100) registered per 511  
 event permitted a crude spectral measurement (four broad 512  
 channels from 20 keV to >300 keV) for each event while the 513  
 distributed sensors with overlapping fields of view permitted 514  
 a rough geolocation of the source. RHESSI on the other 515  
 hand consists of a nine germanium crystals that collect 516  
 photons over  $2\pi$  steradians. RHESSI counts each photon 517

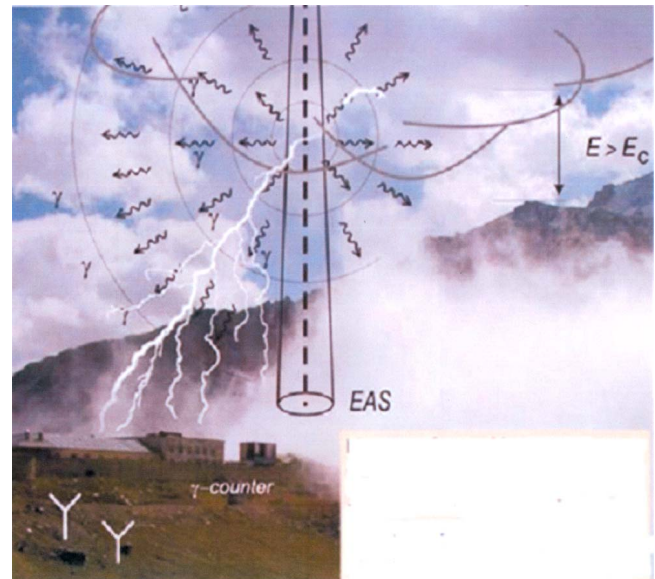


**Figure 9.** Schematics of simultaneous measurements of radio pulses and extensive atmospheric showers conducted at the Tien-Shang Mountain [adapted from *Gurevich and Zybin*, 2005].

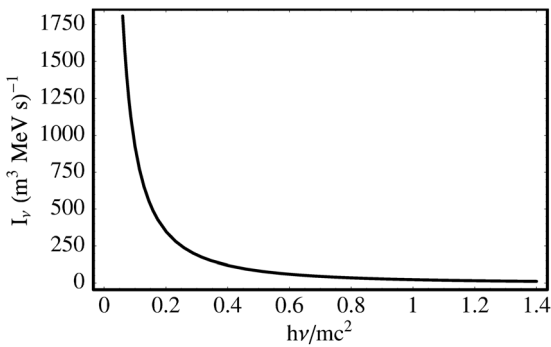


**Figure 10.** Model of spectral density of the bremsstrahlung emission due to RB in thundercloud at 4 km at  $E = 2E_c$  [adapted from Gurevich *et al.*, 1999a].

518 and is able to produce a spectrum from  $\sim 20$  keV to 20 MeV  
 519 with a resolution of up to a few kiloelectron volts. Because  
 520 of the much smaller detector volume however the count rate  
 521 is low (tens of photons per event) and a full spectrum is  
 522 obtained only after summing over tens of events.

523 [33] Cummer *et al.* [2005] found a number of correlations  
 524 between TGF events and VLF signals radiated by lightning.  
 525 The parental lightning had charge moment changes under  
 526 100 C km, which is much smaller than needed to initiate a  
 527 sprite. Interestingly, some TGFs preceded the lightning  
 528 flashes although absence of GPS at RHESSI leads to a  
 529 significant timing inaccuracy. More details can be found in  
 530 the paper by Smith *et al.* [2010].

531 [34] TGFs are thought to be a manifestation of some form  
 532 of RB that develops above a thunderstorm [Bell *et al.*, 1995;  
 533 Inan *et al.*, 1996; Roussel-Dupr e and Gurevich, 1996].  
 534 Nemiroff *et al.* [1997] presented first some temporal and  
 535 spatial characteristics of TGFs measured by BATSE. The  
 536 spectra measured by RHESSI reveal energies up to 30 MeV  
 537 [Smith *et al.*, 2005], in agreement with energies predicted by  
 538 the RB mechanism triggered by cosmic rays [Dwyer and  
 539 Smith, 2005; Carlson *et al.*, 2007; Babich *et al.*, 2007a].  
 540 The time duration of individual events ranges from hundreds  
 541 of microseconds to milliseconds. The geographical distri-  
 542 bution of TGFs roughly corresponds to that of lightning  
 543 over continents at low latitude and also to the distribution of  
 544 sprites [Chen *et al.*, 2005]. However TGF emissions are  
 545 rarely detected over the Southern United States where many  
 546 sprites are observed at ground level [Smith *et al.*, 2005]. The  
 547 energy range from 100 keV to several MeV of the TGF  
 548 spectrum is sensitive to the TGF emission altitude, due to  
 549 the cascading of the high-energy photons to lower energies.  
 550 The analysis of the RHESSI spectra suggests that their  
 551 source is in the range of 15–21 km, implying that thun-  
 552 derstorms and not sprites may initiate TGFs [Dwyer and  
 553 Smith, 2005]. In their recent paper, Hazelton *et al.* [2009]  
 554 used lightning sferics to identify storms near TGFs  
 555 detected by RHESSI. They found that lightning flashes  
 556 closer than 300 km of the subsatellite point produced much  
 557 harder spectrum of TGFs than that located at larger distance.  
 558 Moreover presented in the paper model shows that most  
 559 likely the sources were at 15 km altitude and have a wide-  
 560 beam geometry. Some analyses, however, of BATSE  
 561 spectra have suggested that the source of TGFs could extend

continuously from 15 to 60 km altitude rather than in a 562  
 narrow altitude range [Ostgaard *et al.*, 2006]. More recently 563  
 Ostgaard *et al.* [2006] have addressed dead time issues, 564  
 associated with the BATSE detector, that suggests a pile up 565  
 of high-energy photons. The net result is inference of a 566  
 softer spectrum than actually exists and therefore a higher 567  
 source altitude. Dwyer [2008] analyzed different mechan- 568  
 isms which produce TGFs. He mentioned that RB when 569  
 acting on the external source of cosmic secondary electrons 570  
 is insufficient to account for TGF fluxes. He suggested two 571  
 alternative mechanisms, thermal runaway and relativistic 572  
 feedback. 573

[35] However, those two mechanisms have limited appli- 574  
 cations. Let us consider first the relativistic feedback. 575  
 Figure 12 shows ratio of electron positron pair production 576  
 length ( $l_{\text{pair}}$ ) to the electron avalanche length ( $l_{\text{av}}$ ) for 577  
 two different photon energies 10 MeV (the trace 1) and 578  
 20 MeV (the trace 2). It was computed for STP by using 579  
 the kinetic avalanche time (Figure 3a from this paper) and 580  
 the cross section of electron positron pair production 581  
 [Hubbell *et al.*, 1980]. Figure 12 reveals that at  $\delta_0 > 2$  the 582  
 ratio  $l_{\text{pair}}/l_{\text{av}}$  exceeds 25–30. From the other hand, the size 583  
 of the avalanche region cannot exceed 25–30 avalanche 584  
 lengths, otherwise the electric field causing RB will be 585  
 eliminated. Thus, the mean free path of 10–20 MeV 586  
 photons with respect to pair production exceeds the size of 587  
 avalanche region at  $\delta_0 > 2$ . 588

[36] Therefore, the photons will escape the area of RB, 589  
 and the positrons produced by the high-energy photons 590  
 will not participate in the feedback process. Interesting 591  
 that detailed Monte Carlo computation [Babich *et al.*, 592  
 2005] showed that the positron feedback is negligible at 593  
 $\delta_0 > 3$ , although it plays a significant role at moderate 594  
 field ( $\delta_0 < 2$ ). 595

[37] In order to generate a huge amount of  $\gamma$ -rays such as 596  
 required to produce TGFs, a strong electric field is needed in 597

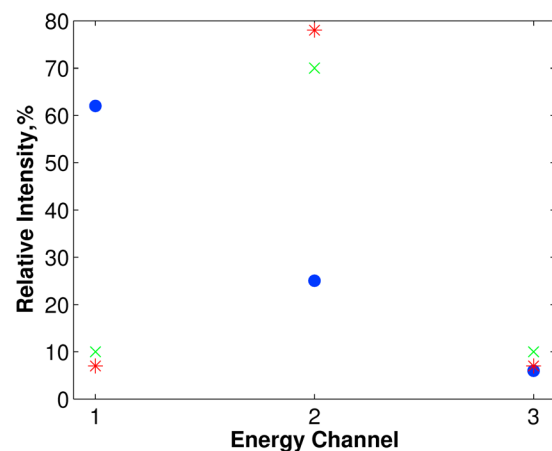


**Figure 11.** The computed energy spectrum for the X-ray emission given in Figure 10. The X-ray fluxes were integrated over three energy channels (30–60, 60–90, and 90–120 keV). The stars show the balloon measurements, the blue points show the spectrum at 70 m from the sources, and the crosses show the spectrum at 420 m from the source. The stars show the balloon measurements by Eack [1996].

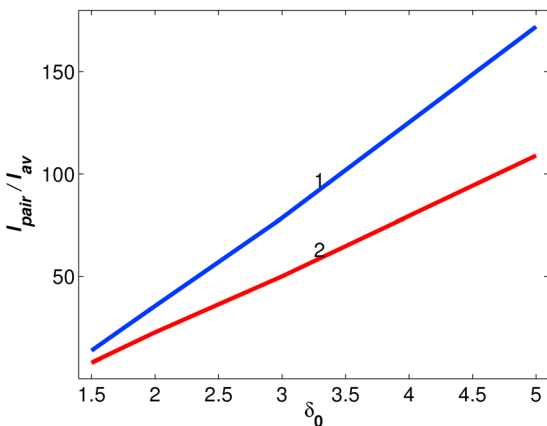


**Figure 12.** The ratio of the pair production length to the avalanche length as a function of  $\delta_0$  computed for two different photon energies 10 MeV (trace 1) and 20 MeV (trace 2).

598 which case the feedback is not playing a role. *Babich et al.*  
 599 [2001b, 2004b, 2008] have addressed this point with  
 600 detailed Monte Carlo simulations and were the first to  
 601 identify the total number of electrons needed to reproduce  
 602 the BATSE and RHESSI measured fluxes. Their simula-  
 603 tions assumed an average figure for the background of  
 604 seed energetic electrons and did not include the effects of  
 605 either thermal runaway or feedback. However, a moderate  
 606 field supplemented by the feedback mechanism could still  
 607 play a role in the TGF production, but it requires that RB  
 608 occurs in a thick layer having a vertical scale of a few  
 609 kilometers. Therefore, we agree with the conclusion made  
 610 by *Babich et al.* [2005] that “significantly more work is  
 611 required to establish the existence and role of feedback in  
 612 RB under thunderstorm electrical conditions”.

613 [38] The thermal runaway has its own limitations,  
 614 namely it requires enormous electric fields which can be  
 615 formed only on a short spatial scale such as in a streamer  
 616 tip, although it can be involved in the production of TGFs  
 617 in conjunction with RB. Furthermore extensive atmo-  
 618 spheric showers can play an important role in TGF pro-  
 619 duction [*Gurevich et al.*, 2004a]. Although *Dwyer* [2008]  
 620 does not share this idea because he believes it is not  
 621 supported by the time structures and fluencies of TGFs. It  
 622 should be noted that the reliability of the models of the  
 623 time structures of a few tens of photons scattering through  
 624 the entire atmosphere is quite limited.

625 [39] Further work is needed to evaluate the effect of  
 626 summing multiple RHESSI events to obtain a spectrum and  
 627 the corresponding impact on determination of a source  
 628 altitude. The possibility of two kinds of TGFs correspond-  
 629 ing to low- and high-altitude sources cannot be completely  
 630 ruled out. A lightning leader as a source of TFFs is pre-  
 631 dicted by *Moss et al.* [2006], who show that thermal elec-  
 632 trons can be accelerated in the leader streamer zone up to  
 633 energies of several hundreds of kiloelectron volts and pos-  
 634 sibly up to several tens of MeV. This mechanism then  
 635 predicts that some TGFs can be produced by high-altitude  
 636 lightning processes. The region from 15 to 21 km lies just  
 637 above thunderstorm cloud tops where a screening layer of  
 638 charge forms and the question of how a runaway discharge

forms or emerges from the cloud into this region to produce  
 bremsstrahlung photons (or TGFs) was addressed in the  
 above cited theoretical works related to sprites and predicted  
 by *Yukhimuk et al.* [1998] in discussing blue jets. *Gurevich*  
*et al.* [2004c] proposed a mechanism of TGF generation  
 by joint effect of RB and EAS. *Milikh et al.* [2005] men-  
 tioned that when RB occurs at the height  $z > 15\text{--}20$  km the  
 relativistic electrons are magnetized, and their trapping can  
 promote propagation of the electromagnetic pulse associated  
 with thunderstorms as a whistler mode. Much work remains  
 to either confirm previous work or identify the actual source  
 of TGFs.

[40] Important theoretical models of TGFs were presented  
 by the Stanford group, who discussed TGF production by  
 RB due to quasi-electrostatic thundercloud fields [*Lehtinen*  
*et al.*, 1996, 1999, 2001], as well as by the return stroke  
 from lightning [*Inan and Lehtinen*, 2005].

### 3.3. $\gamma$ Bursts Due to Lightning Stepped Leaders

[41] So far, we discussed high-energy radiation generated  
 by the RB which precedes lightning flashes although the  
 ground based observations showed that lightning itself can  
 also be a source of  $\gamma$ -rays. *Moore et al.* [2001] first reported  
 X-rays associated with lightning stepped leaders. This  
 experimental result was supported by *Dwyer* [2003], who  
 detected X-ray bursts in the range 30–250 keV with a typi-  
 cal duration of less than 1  $\mu$ s. It was assumed that the  
 source of those bursts are the electric field changes  
 accompanying stepping of the leader [*Dwyer et al.*, 2005].  
 Recently *Howard et al.* [2008] experimentally proved that  
 the sources of X-rays are collocated in space with the leader  
 step electric field changes. Besides, the X-rays were delayed  
 by 0.1–1.3  $\mu$ s with respect to those field changes. The delay  
 shows the time needed to develop the RB.

[42] Theory which described this effect was introduced  
 by *Moss et al.* [2006] and *Gurevich et al.* [2007]. Inter-  
 estingly these two groups used different methods (analytical  
 model by *Gurevich* and Monte Carlo model by *Moss*) but  
 came to similar conclusions. Namely, that in a streamer tip  
 such as in a streamer zone of lightning leader where the  
 electric field can reach 150 kV/cm, a thermal runaway  
 could occur which can accelerate electrons up to a few  
 kiloelectron volts. Those electrons could in turn trigger RB  
 instead of relativistic seed electrons due to galactic cosmic  
 rays. The estimates show that a significant amount of  
 thermal runaway electrons  $N_R = \int S_R V dt \simeq 3 \times 10^{12} e\lambda$   
 can be produced in a small volume  $V = 10 \text{ cm} \times 3 \text{ cm}^2$   
 within  $dt = 0.3 \mu$ s. Note that in RB the spatial size scales as  
 $\lambda_{av} = \lambda_{av}^0 / \delta^2$ ,  $\delta = E/E_c = 70\text{--}100$ . Thus  $\lambda_{av}$  could be as low  
 as a few centimeters and thus can be developed in a  
 streamer zone of a lightning stepped leader.

[43] Furthermore, the model [*Gurevich et al.*, 2007]  
 shows that  $\gamma$ -ray emission generated by the RB due to a  
 single lightning step can reach energies of 0.01–1 kJ over  
 0.1–0.5  $\mu$ s. Thus for 2–50 steps the  $\gamma$ -burst can reach an  
 energy of 1–10 kJ. Finally, such a RB generates currents  
 of 0.3–5 kA, which is in line with the observations of  
 lightning stepped leaders.

### 3.4. Neutron Bursts Due to Lightning

[44] The possible significance of neutron production by  
 lightning was noted by *Fleischer et al.* [1974]. Not only does

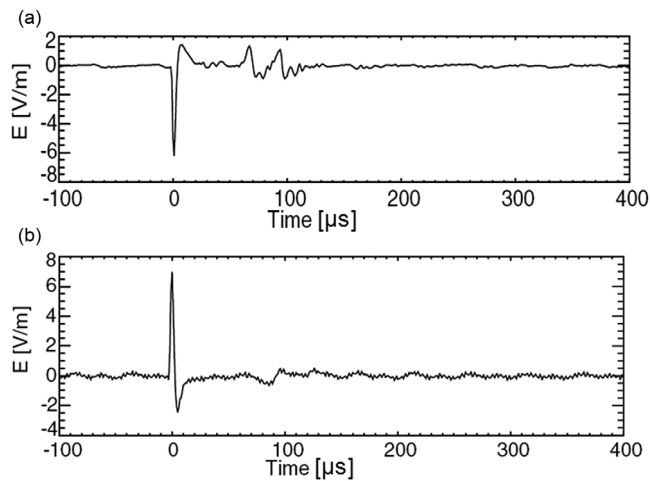


**Figure 13.** (a) Positive NBP and (b) negative NBP observed by Los Alamos Sferic Array adapted from *Smith et al.* [2002].

699 the generation of neutrons provide valuable information  
700 about the discharge mechanism itself but an enhanced neu-  
701 tron flux would also have important consequences for  $^{14}\text{C}$   
702 dating through the neutron capture reaction  $n(^{14}\text{N}, ^{14}\text{C})^1\text{H}$ .  
703 The implications of the latter are that the ages of various  
704 materials would be underestimated unless the historical  
705 occurrence rate and geographical distribution of lightning  
706 were taken into consideration.

707 [45] The first estimates of neutron yield from lightning  
708 were obtained by scaling the reaction  $^2\text{H}(^2\text{H},n)^3\text{He}$  in elec-  
709 trical explosions of nylon threads enriched by deuterium  
710 [Libby and Lukens, 1973; Stephanakis et al., 1972]. Fleisher  
711 et al. [1974] then performed neutron-monitoring experi-  
712 ments in association with laboratory discharges that simu-  
713 lated the plasma conditions thought to exist in the lightning  
714 channel. They found no evidence for neutron production but  
715 instead set upper limits on the number of neutrons generated  
716 by lightning to  $4 \times 10^8$  thermal neutrons and/or  $7 \times 10^{10}$   
717 2.45 MeV neutrons per flash.

718 [46] The first direct measurements of the neutron flux in  
719 the thunderstorm environment [Fleisher, 1975] yielded null  
720 results. Positive results were not obtained until 10 years  
721 later [Shah et al., 1985] when Shah and his colleagues  
722 reported observing statistically significant enhancements in  
723 the neutron flux in correlation with thunderstorm EMP.  
724 They estimated the average neutron yield to range from  
725  $10^7$  to  $10^{10}$  neutrons per lightning discharge assuming the  
726 reaction  $^2\text{H}(^2\text{H},n)^3\text{He}$  with neutron energy  $\epsilon_n = 2.45$  MeV.  
727 From the measured delay times relative to EMP they  
728 deduced plausible yields extending to  $2 \times 10^{12}$  assuming  
729  $\epsilon_n$  as low as 0.023 eV. Shyam and Kaushik [1999] and  
730 Kuzhewskij [2004] have also communicated statistically  
731 significant single events, in which neutron bursts associ-  
732 ated with atmospheric lightning discharges were detected  
733 near sea level in India and Moscow. Results of these  
734 successful experiments were interpreted as stemming from  
735 the nuclear fusion reaction  $^2\text{H}(^2\text{H},n)^3\text{He}$  within the light-  
736 ning channel.

737 [47] Recently, Babich and Roussel-Dupré [2007] showed  
738 that the prevailing neutron generation theory based on

synthesis of deuterium nuclei in the lightning channel is not 739  
feasible. Instead, this phenomenon is most likely connected 740  
with photonuclear reactions ( $\gamma, n$ ) associated with an elec- 741  
trical breakdown driven by relativistic runaway electrons 742  
(i.e., RB). Neutron production by photonuclear reactions in 743  
air requires photon energies exceeding 10 MeV, a value 744  
that is consistent with the upper energies of the brems- 745  
strahlung spectrum produced in a runaway breakdown 746  
avalanche. The neutron yield of photonuclear reactions that 747  
accompany atmospheric  $\gamma$ -ray bursts associated with 748  
lightning discharges of various forms was estimated by 749  
*Babich and Roussel-Dupré* [2007] to lie between  $\sim 10^{13}$  750  
and  $10^{15}$  per discharge. More detailed calculations are 751  
presented by *Babich et al.* [2007a, 2007b, 2008]. 752

### 3.5. Narrow Bipolar Pulses

[48] Narrow bipolar pulses (NBP) are the electromagnetic 754  
signature of a distinct class of impulsive and energetic 755  
intracloud discharges that occur in some thunderstorms. 756  
NBP were observed by broadband field-change antennas 757  
[*Smith et al.*, 2002; *Eack*, 2004] and by the FORTE satellite 758  
[*Jacobson*, 2003]. They are characterized by strong VHF 759  
emission having peak power 100–300 GW and bipolar 760  
waveforms. A positive polarity NBP exhibits a radiation 761  
field waveform that begins as a positive electron field peak, 762  
while followed by a negative overshoot. A negative polarity 763  
NBP begins as a negative electric field peak followed by a 764  
positive overshoot (see Figure 13). This indicates that a 765  
positive NBP results from a dipole discharge in which 766  
positive charge is located over negative charge, while a 767  
negative NBP results from an inverted dipole with a neg- 768  
ative charge over positive. The positive NBP are scattered 769  
between 15 and 20 km, while their spatial distribution 770  
peaks at 17 km. The negative NBP are spread between 7 771  
and 15 km, with the distribution peak at 13 km [*Smith* 772  
*et al.*, 2002]. 773

[49] NBP has a mean duration of 5–10  $\mu$ s with full width at 774  
half maximum 2–5  $\mu$ s and mean relaxation time of 2–5  $\mu$ s. 775  
An average NBP has a peak current of 30–100 kA, while the 776  
corresponding dipole moment changes up to 2 C km. The 777  
discharges responsible for NBP propagate at an average 778  
velocity of  $1.5 \times 10^8$  m/s [*Eack*, 2004]. 779

[50] NBP is observed in the frequency range 200–500 kHz. 780  
The amplitude of the effective electric field at the distance 781  
 $R$  from the source is  $E \sim 10 - 30 \left(\frac{100 \text{ km}}{R}\right) \text{V/m}$ . Notice that 782  
NBP is always accompanied by intensive radio emission in a 783  
wide frequency range up to 500 MHz. Detailed studies of 784  
HF emission in the frequency range 26–48 MHz conducted 785  
by the FORTE satellite [*Jacobson*, 2003] found that this 786  
emission has an integrated ERP  $\geq 40$  kW. It was related to 787  
a strong intracloud pulse. These pulses are accompanied by 788  
an optical emission with an intensity 2 orders of magnitude 789  
less than that in conventional flashes. Finally there are 790  
indications that NBP have been correlated with TGF 791  
[*Stanley et al.*, 2006; *Shah et al.*, 1985]. 792

[51] *Jacobson* [2003] was the first to suggest that NBP 793  
have relevance to RB, while the first quantitative model 794  
of NBP was presented by *Gurevich and Zybin* [2004]. 795  
According to this model NBP are generated by runaway 796  
breakdown triggered by extensive atmospheric shower. 797  
The latter is caused by cosmic particle having energy 798

799  $10^{14}$ – $10^{19}$  eV. This type of very intensive RB was termed  
800 RB-EAS.

801 [52] The presented model successfully explained the  
802 observed time scales of RB-EAS. In fact, at the altitudes of  
803 interest the avalanche time is of about 1–5  $\mu$ s, which fits well  
804 with the NBP rise time. The fall of NBP corresponds to the  
805 relaxation of the runaway discharge, which is due to the  
806 electron attachment to molecular oxygen in triple collisions.  
807 The electron attachment time is  $\tau_{\text{att}} \sim (5 \times 10^{18} \text{ cm}^{-3}/\text{Nm})^2 \mu$ s.  
808 For the considered height range 13–18 km the value of  $\tau_{\text{att}}$   
809 fits well with the observed fall time of NBP.

810 [53] The electric current generated by RB-EAS discharge  
811 is unipolar. For given external field, its maximum is pro-  
812 portional to the number of thermal electrons, which in turn  
813 is proportional to the number of runaway electrons deter-  
814 mined by the energy of the cosmic ray particle. As shown by  
815 *Gurevich and Zybin* [2004], the current is  $J_m \sim (\epsilon_p/10^{17} \text{ eV})$   
816 kA. This current emits the bipolar radio pulse.

817 [54] Notice that the size of the pulsed current region is  
818 determined by the EAS scale length of 300–400 m, which is  
819 less than the wavelength  $\lambda = 600$ – $1500$  m of the NBP radi-  
820 ated VLF emission with the frequency 200–500 kHz.  
821 Therefore the VLF emission is radiated coherently, its power  
822  $P = 2J^2/3c$  is growing as  $J^2$ , and it can reach 100–300 GW.  
823 Respectively the energy of such pulses can reach MJ. In  
824 contrast to the coherent VLF emission, the HF emission from  
825 NBP is incoherent, its power is less than 10 MW, and the  
826 radiated energy does not exceed 100 J.

827 [55] Recently *Dwyer et al.* [2009] claimed that according  
828 to their estimates the model [*Gurevich and Zybin*, 2004;  
829 *Gurevich et al.*, 2004c] requires either unrealistically high-  
830 electron avalanche multiplication or ultrahigh-energy air  
831 showers. Thus, the subject requires more theoretical studies.

#### 832 4. Conclusions

833 [56] The introduction of runaway breakdown and its  
834 potential initiation by cosmic rays to our studies of lightning  
835 and the thunderstorm electrical environment has provided  
836 us with an entirely new perspective on how the Earth’s  
837 atmosphere couples to the cosmos. In many respects our  
838 atmosphere can be thought of as a giant scintillator or  
839 “cloud” chamber that is continuously lit up by the passage  
840 of energetic radiation from space. Thunderstorms provide  
841 an electrically active region that can locally enhance the RF  
842 and optical output of the atmospheric scintillator in a daz-  
843 zling display, one that has fascinated man for millennia.  
844 Indeed Wilson would have been proud to see us return to  
845 his original ideas and to his invention as a metaphorical if  
846 not scientifically useful substitute for the Earth’s atmo-  
847 sphere. This notion has far reaching implications both for  
848 the potential utility of lightning as a diagnostic to probe  
849 the mysteries of energetic cosmic ray showers and therefore  
850 the universe and for understanding the very nature of the  
851 lightning discharge and its effects on the atmosphere and  
852 human activity.

853 [57] Runaway breakdown could have manifestations in  
854 many planetary and astrophysical phenomena and yet we  
855 are only beginning to unravel how it actually operates in the  
856 natural environment or how it is initiated. Because of its  
857 intrinsically large scales (tens to hundreds of meters at  
858 atmospheric pressure) the mechanism is very difficult to

produce in existing laboratory configurations. On the other 859  
hand immense electrical generators such as thunderstorms 860  
do provide the requisite conditions and there is every 861  
indication that this process is at work in many forms of 862  
lightning. 863

[58] But is this picture correct or even partially so? The 864  
question of what we know so far about RB was addressed in 865  
some detail in this paper. But where do we go from here? 866

#### 5. Some Outstanding Issues 867

[59] A great deal of progress has been made in the last 868  
decade and a half on our basic understanding of RB and its 869  
potential role in affecting thunderstorm electrical activity 870  
and in initiating or driving lightning discharges of various 871  
types including stepped leaders, intracloud lightning, and 872  
high-altitude discharges. Both theory and observation have 873  
worked together over the years, one guiding and/or correct- 874  
ing the other, to provide an emerging, albeit rudimen- 875  
tary, image of how nature operates in the thunderstorm 876  
environment. Much scientific research remains however 877  
before the picture is completed. Some of the outstanding 878  
issues that merit further investigation include the following: 879

[60] 1. A comprehensive model for TGF generation is 880  
needed which should include three main elements, and 881  
should address some relevant questions: (1) description of 882  
RB based on a kinetic model; (2) self-consistent description 883  
of the thundercloud electrodynamics, namely, how the 884  
thunderstorm electric field affects RB, including the feed- 885  
back due to electron avalanche which produces charge 886  
separation; and (3) model of generation of  $\gamma$ -rays due to RB 887  
and their propagation in the atmosphere. 888

[61] Among the questions that arise with regards to TGFs 889  
are as follows: (1) What role is played by EAS? (2) What 890  
role is played by meteorology, namely what geographic 891  
locations are preferential for TGF generation, and is there an 892  
optimal height for generating TGF? (3) Can TGFs be initi- 893  
ated at the height where relativistic electrons become mag- 894  
netized? In this case the effects due to the geomagnetic field 895  
should be taken into account. (4) Are TGFs and NBPs 896  
related? (5) Do red sprites or blue jets produce TGFs? (5) 897  
Are TNFs produced in conjunction with TGFs? 898

[62] 2. A model for  $\gamma$ -bursts produced in stepped leaders is 899  
needed which should include two main elements and should 900  
address some relevant questions: (1) kinetic theory of RB at 901  
high electric field  $E/E_c > 10$  and (2) theoretical description of 902  
stepped leaders including model of the formation of self- 903  
consistent governing fields [see *Raizer et al.*, 2010]. 904

[63] Questions include the following: (1) Is there a feed- 905  
back between RB and leader formation? (2) Is the electric 906  
field formed in the stepped leader sufficient to cause RB? 907

[64] Solution of the above problems will require theoretical 908  
and experimental efforts. 909

[65] 3. The feedback mechanism identified by Dwyer 910  
needs further elaboration in the context of the thunderstorm 911  
environment and the presence of EAS: Self-consistent 912  
electromagnetic and kinetic calculations with the thunder- 913  
storm electric field, EAS initiation, RB, and feedback 914  
included are needed. 915

[66] Relevant questions include the following: (1) If 916  
feedback limits the thunderstorm electric field to the 917  
threshold for RB then why do we observe lightning at all? 918

919 (2) Are the electrical conditions in the thunderstorm such  
 920 that a strong RB develops before feedback can limit the  
 921 field? (3) Do EAS locally enhance the ambient thunderstorm  
 922 field sufficiently to initiate a discharge?  
 923 [67] 4. High current discharges and development of  
 924 plasma instabilities: A detailed kinetic theory for the  
 925 development of RB at high current levels has yet to be  
 926 developed and is needed.  
 927 [68] Relevant questions include the following: (1) What are  
 928 the current levels achieved in an RB discharge? (2) Are they  
 929 sufficient to drive plasma instabilities? (3) What instabilities  
 930 develop? (4) Are they observed in lightning discharges?

931 [69] **Acknowledgments.** We appreciate valuable discussions with  
 932 Professor Alex Gurevich.  
 933 [70] Zuyin Pu thanks Jeff Morrill and the other reviewers for their  
 934 assistance in evaluating this paper.

### 935 References

- 936 Alexeenko, V. V., N. S. Khaerdinov, A. S. Lidvansky, and V.B. Petkov  
 937 (2002), Transient variations of secondary cosmic rays due to atmospheric  
 938 electric field and evidence for pre-lightning particle acceleration, *Phys.*  
 939 *Lett. A*, *301*, 299–306.
- 940 Babich, L. P., I. M. Kutsyk, E. N. Donskoy, and A. Yu. Kudryavtsev  
 941 (1998), *Phys. Lett. A*, *245*, 460.
- 942 Babich, L. P., et al. (2001a), Comparison of relativistic runaway electron  
 943 avalanche rates obtained from Monte Carlo simulations and kinetic equation  
 944 solution, *IEEE Trans. Plasma Sci.*, *29*, 430–438.
- 945 Babich, L. P., R. I. Il'kayev, A. Yu. Kudryavtsev, I. M. Kutsyk, and  
 946 R. A. Roussel-Dupre (2001b), Analysis of  $\gamma$ -ray pulses of the atmo-  
 947 spheric origin recorded aboard the orbital station, *Dokl. Earth Sci.*, *381*(8),  
 948 994–997. (*Dokl. Akad. Nauk*, *381*, 247–250)
- 949 Babich, L. P., et al. (2004a), An experimental investigation of an avalanche  
 950 of relativistic runaway electrons under normal conditions, *High Temp.*,  
 951 *42*(1), 1–11.
- 952 Babich, L. P., E. N. Donskoj, I. M. Kutsyk, and R. A. Roussel-Dupre  
 953 (2004b), Bremsstrahlung of relativistic electron avalanche in the atmo-  
 954 sphere, *Geomagn. Aeron.*, *44*(5), 254.
- 955 Babich, L. P., E. N. Donskoy, I. M. Kutsyk, and R. A. Roussel-Dupre  
 956 (2005), The feedback mechanism of runaway air breakdown, *Geophys.*  
 957 *Res. Lett.*, *32*, L09809, doi:10.1029/2004GL021744.
- 958 Babich, L. P., and R. A. Roussel-Dupré (2007), Origin of neutron flux  
 959 increases observed in correlation with lightning, *J. Geophys. Res.*,  
 960 *112*, D13303, doi:10.1029/2006JD008340.
- 961 Babich, L. P., A. Y. Kudryavtsev, M. L. Kudryavtseva, and I. M. Kutsyk  
 962 (2007a), Neutron generation by upward atmospheric discharges, *Dokl.*  
 963 *Earth Sci.*, *415A*, 885–889.
- 964 Babich, L. P., A. Y. Kudryavtsev, M. L. Kudryavtseva, and I. M. Kutsyk  
 965 (2007b), Terrestrial  $\gamma$ -ray flashes and neutron pulses from direct simula-  
 966 tions of gigantic upward atmospheric discharge, *Sov. Phys. JETP, Engl.*  
 967 *Transl.*, *85*, 483–487.
- 968 Babich, L. P., A. Y. Kudryavtsev, M. L. Kudryavtsev, and I. M. Kutsyk  
 969 (2008), Atmospheric  $\gamma$ -ray and neutron flashes, *Sov. Phys. JETP, Engl.*  
 970 *Transl.*, *106*, 65–76.
- 971 Bell, T. F., V. P. Pasko, and U. S. Inan (1995), Runaway electrons as a  
 972 source of red sprites in the mesosphere, *Geophys. Res. Lett.*, *22*(16),  
 973 2127–2130, doi:10.1029/95GL02239.
- 974 Bethe, H. A., and J. Ashkin (1953), Passage of radiations through matter, in  
 975 *Experimental Nuclear Physics*, vol. 1, edited by E. Segre, pp. 166–357,  
 976 Wiley, New York.
- 977 Brown, S. C. (1959), *Basic Data of Plasma Physics*, John Wiley, New  
 978 York.
- 979 Brown, S. C. (1966), *Introduction to Electrical Discharges in Gases*, John  
 980 Wiley, New York.
- 981 Carlson, B. E., N. G. Lehtinen, and U. S. Inan (2007), Constraints on ter-  
 982 restrial  $\gamma$ -ray flash production from satellite observation, *Geophys. Res.*  
 983 *Lett.*, *34*, L08809, doi:10.1029/2006GL029229.
- 984 Chen, B., et al. (2005), Global distribution and seasonal distribution varia-  
 985 tion of transient luminous events, *Eos Trans. AGU*, *86*(52), Fall Meet.  
 986 Suppl., Abstract AE23A-0991.
- 987 Colman, J. J., R. A. Roussel-Dupré, and L. Triplett (2010), Temporally  
 988 self-similar electron distribution functions in atmospheric breakdown:  
 The thermal runaway regime, *J. Geophys. Res.*, *115*, A00E16, 989  
 doi:10.1029/2009JA014509. 990
- Cummer, S. A., Y. Zhai, W. Hu, D. M. Smith, L. I. Lopez, and M. A. Stanley  
 (2005), Measurements and implications of the relationship between light-  
 992 ning and terrestrial  $\gamma$ -ray flashes, *Geophys. Res. Lett.*, *32*, L08811, 993  
 doi:10.1029/2005GL022778. 994
- D'Angelo, N. (1987), On X-rays from thunderclouds, *Ann. Geophys., Ser.*  
*B*, *5*, 119–122. 995
- Dreicer, H. (1960), Electron and ion runaway in a fully ionized gas: II, 996  
*Phys. Rev.*, *117*, 329–342. 997
- Dwyer, J. R. (2003), A fundamental limit on electric fields in air, *Geophys.*  
*Res. Lett.*, *30*(20), 2055, doi:10.1029/2003GL017781. 1000
- Dwyer, J. R., et al. (2004), Measurements of X-ray emission from rocket-  
 1001 triggered lightning, *Geophys. Res. Lett.*, *31*, L05118, doi:1029/  
 2003GL018770. 1002
- Dwyer, J. R. (2005), The initiation of lightning by runaway air breakdown, 1003  
*Geophys. Res. Lett.*, *32*, L20808, doi:1029/2005GL023975. 1004
- Dwyer, J. R., and D. M. Smith (2005), A comparison between Monte Carlo 1005  
 simulations of runaway breakdown and terrestrial  $\gamma$ -ray flash observa- 1006  
 tions, *Geophys. Res. Lett.*, *32*, L22804, doi:10.1029/2005GL023848. 1007
- Dwyer, J. R., H. K. Rassul, Z. Saleh, M. A. Uman, J. Jerauld, and 1008  
 J. A. Plumer (2005), X-ray bursts produced by laboratory sparks in air, 1009  
*Geophys. Res. Lett.*, *32*, L20809, doi:10.1029/2005GL024027. 1010
- Dwyer, J. R. (2008), Source mechanism of terrestrial  $\gamma$ -ray flashes, *J. Geo-*  
*phys. Res.*, *113*, D10103, doi:10.1029/2007JD009248. 1011
- Dwyer, J. R., M. A. Uman, and H. K. Rassul (2009), Remote measurements 1012  
 of thundercloud electrostatic fields, *J. Geophys. Res.*, *114*, D09208, 1013  
 doi:10.1029/2008JD011386. 1014
- Eack, K. B. (1996), Balloon-borne X-ray spectrometer for detection of 1015  
 X-rays produced by thunderstorms, *Rev. Sci. Instrum.*, *67*, 2005–2009. 1016
- Eack, K. B., W. H. Beasley, W. D. Rust, T. C. Marshall, and M. Stolzenburg 1017  
 (1996), X-ray pulses observed above a mesoscale convective system, 1018  
*Geophys. Res. Lett.*, *23*(21), 2915–2918, doi:10.1029/96GL02570. 1019
- Eack, K. B., D. M. Suszcynsky, W. H. Beasley, R. Roussel-Dupre, and 1020  
 E. Symbalisty (2000),  $\gamma$ -ray emissions observed in a thunderstorm anvil, 1021  
*Geophys. Res. Lett.*, *27*(2), 185–188, doi:10.1029/1999GL010849. 1022
- Eack, K. B. (2004), Electrical characteristics of narrow bipolar events, *Geo-*  
*phys. Res. Lett.*, *31*, L20102, doi:10.1029/2004GL021117. 1023
- Feldman, W. C., E. M. D. Symbalisty, and R. A. Roussel-Dupre (1996a), 1024  
 Hard X ray survey of energetic electrons from low-Earth orbit, *J. Geo-*  
*phys. Res.*, *101*(A3), 5195–5209, doi:10.1029/95JA03393. 1025
- Feldman, W. C., E. M. D. Symbalisty, and R. A. Roussel-Dupre 1026  
 (1996b), Survey of discrete hard X-ray enhancements observed from 1027  
 low-Earth orbit, *J. Geophys. Res.*, *101*(A3), 5211–5217, doi:10.1029/  
 95JA03394. 1028
- Fishman, G. J., et al. (1994), Discovery of intense  $\gamma$ -ray flashes of atmo- 1029  
 spheric origin, *Science*, *264*, 1313–1316. 1030
- Fleisher, R. L., J. A. Plumer, and K. Crouch (1974), Are neutrons generated 1031  
 by lightning?, *J. Geophys. Res.*, *79*(33), 5013–5017, doi:10.1029/  
 JC079i033p05013. 1032
- Fleisher, R. L. (1975), Search for neutron generation by lightning, *J. Geo-*  
*phys. Res.*, *80*(36), 5005–5009, doi:10.1029/JC080i036p05005. 1033
- Gurevich, A. V. (1961), On the theory of runaway electrons, *J. Exp. Theor.*  
*Phys.*, *12*, 904–912. 1034
- Gurevich, A. V., G. M. Milikh, and R. Roussel-Dupre (1992), Runaway 1035  
 electron mechanism of air breakdown and preconditioning during a thun- 1036  
 derstorm, *Phys. Lett. A*, *165*, 463–467. 1037
- Gurevich, A. V., G. M. Milikh, and R. Roussel-Dupre (1994), Nonuniform 1038  
 runaway air-breakdown, *Phys. Lett. A*, *187*, 197–201. 1039
- Gurevich, A. V., J. A. Valdivia, G. M. Milikh, and K. Papadopoulos 1040  
 (1996), Runaway electrons in the atmosphere in the presence of a mag- 1041  
 netic field, *Radio Sci.*, *31*(6), 1541–1554, doi:10.1029/96RS02441. 1042
- Gurevich, A. V., G. M. Milikh, and J. A. Valdivia (1997a), Model of X-ray 1043  
 emission and fast preconditioning during a thunderstorm, *Phys. Lett. A*, 1044  
*231*, 402–408. 1045
- Gurevich, A. V., N. D. Borisov, and G. M. Milikh (1997b), *Physics of*  
*Microwave Discharges, Artificially Ionized Regions in the Atmosphere,* 1046  
 Gordon and Breach, U. K. 1047
- Gurevich, A. V., and G. M. Milikh (1999), Generation of X-rays due to 1048  
 multiple runaway breakdown inside thunderclouds, *Phys. Lett. A*, *262*, 1049  
 457–463. 1050
- Gurevich, A. V., K. P. Zybin, and R. A. Roussel-Dupre (1999a), Lightning 1051  
 initiation by simultaneous effect of runaway breakdown and cosmic ray 1052  
 showers, *Phys. Lett. A*, *254*, 79–97. 1053
- Gurevich, A. V., K. F. Sergeichev, I. A. Sychoy, R. Roussel-Dupre, and K. 1054  
 P. Zybin (1999b), First observations of runaway breakdown phenomenon 1055  
 in laboratory experiments, *Phys. Lett. A*, *260*(3–4), 269–278. 1056
- Gurevich, A. V., and K. P. Zybin (2001), Runaway breakdown and electric 1057  
 discharges in thunderstorms, *Phys. Uspekhi*, *44*, 1119–1140. 1058  
 1059  
 1060  
 1061  
 1062  
 1063  
 1064  
 1065  
 1066  
 1067

- 1068 Gurevich, A. V., L. M. Duncan, A. N. Karashtin, and K. P. Zybin (2003),  
 1069 Radio emission of lightning initiation, *Phys. Lett. A*, 312(3–4), 228–237.  
 1070 Gurevich, A. V., et al. (2004a), Experimental evidence of giant electron- $\gamma$ -  
 1071 bursts generated by extensive atmospheric showers in thunderclouds,  
 1072 *Phys. Lett. A*, 325(5–6), 269–278.  
 1073 Gurevich, A. V., Y. V. Medvedev, and K. P. Zybin (2004b), Thermal elec-  
 1074 trons and electric current generated by runaway breakdown effect, *Phys.*  
 1075 *Lett. A*, 321, 179–184.  
 1076 Gurevich, A. V., Y. V. Medvedev, and K. P. Zybin (2004c), A new type of  
 1077 discharge generated in thunderclouds by joint action of runaway break-  
 1078 down and extensive atmospheric shower, *Phys. Lett. A*, 329, 348–361.  
 1079 Gurevich, A. V., and K. P. Zybin (2004), High-energy cosmic ray particles  
 1080 and the most powerful discharges in thunderstorm atmosphere, *Phys.*  
 1081 *Lett. A*, 329, 341–347.  
 1082 Gurevich, A. V., and K. P. Zybin (2005), Runaway breakdown and the  
 1083 mysteries of lightning, *Phys. Today*, 58, 37–43.  
 1084 Gurevich, A. V., K. P. Zybin, and Y. V. Medvedev (2007), Runaway  
 1085 breakdown in strong electric field as a source of terrestrial  $\gamma$ -flashes  
 1086 and  $\gamma$ -bursts in lightning leader steps, *Phys. Lett. A*, 361, 119–125.  
 1087 Gurevich, A. V., et al. (2009), Effect of cosmic rays and runaway break-  
 1088 down on lightning discharges, *Phys. Uspekhi*, 179, doi:10.3367/  
 1089 UFN0179.200907h.0779.  
 1090 Hazelton, B. J., B. W. Grefenstette, D. M. Smith, J. R. Dwyer, X. M. Shao,  
 1091 S. A. Cummer, T. Chronis, E. H. Lay, and R. H. Holzworth (2009), Spec-  
 1092 tral dependence of terrestrial  $\gamma$ -ray flashes on source distance, *Geophys.*  
 1093 *Res. Lett.*, 36, L01108, doi:10.1029/2008GL035906.  
 1094 Hill, R. D. (1963), Investigation of electron runaway in lightning, *J. Geo-*  
 1095 *phys. Res.*, 68, 6261–6266.  
 1096 Howard, J., et al. (2008), Co-location of lightning leader X-ray and electric  
 1097 field change sources, *Geophys. Res. Lett.*, 35, L13817, doi:10.1029/  
 1098 2008GL034134.  
 1099 Hubbell, J. H., H. A. Gimm, and I. Ferbf (1980), Pair, triplet, and total  
 1100 atomic cross sections (and mass attenuation coefficients) for 1 MeV–  
 1101 100 GeV photons in elements  $Z = 1$  to 100, *J. Phys. Chem. Ref. Data*,  
 1102 9(4), 1023–1147.  
 1103 Inan, U. S., and N. G. Lehtinen (2005), Production of terrestrial  $\gamma$ -ray  
 1104 flashes by an electromagnetic pulse from a lightning return stroke, *Geo-*  
 1105 *phys. Res. Lett.*, 32, L19818, doi:10.1029/2005GL0237032.  
 1106 Inan, U. S., S. C. Reising, G. L. Fishman, and J. M. Horack (1996), On the  
 1107 association of terrestrial  $\gamma$ -ray bursts with lightning and implications for  
 1108 sprites, *Geophys. Res. Lett.*, 23(9), 1017–1020, doi:10.1029/96GL00746.  
 1109 Jacobson, A. R. (2003), How do the strongest radio pulses from thunder-  
 1110 storms relate to lightning flashes?, *J. Geophys. Res.*, 108, 4778,  
 1111 doi:10.1029/2003JD003936.  
 1112 Kroll, N., and K. M. Watson (1972), Theoretical study of ionization of air  
 1113 by intense laser pulse, *Phys. Rev. A*, 5, 1883–1905.  
 1114 Kuzhewskij, B. M. (2004), Neutron generation in lightning, *Phys. Astron-*  
 1115 *omy*, 5, 14–16.  
 1116 Lebedev, A. N. (1965), Contribution to the theory of runaway electrons,  
 1117 *J. Exp. Theor. Phys.*, 21, 931–933.  
 1118 Lehtinen, N. G., N. Walt, T. F. Bell, U. S. Inan, and V. P. Pasko (1996),  
 1119  $\gamma$ -ray emission produced by a relativistic beam of runaway electrons  
 1120 accelerated by quasi-electrostatic thundercloud fields, *Geophys. Res.*  
 1121 *Lett.*, 23(19), 2645, doi:10.1029/96GL02573.  
 1122 Lehtinen, N. G., T. F. Bell, and U. S. Inan (1999), Monte Carlo simulation  
 1123 of runaway MeV electron breakdown with application to red sprites and  
 1124 terrestrial  $\gamma$ -ray flashes, *J. Geophys. Res.*, 104(A11), 24,699–24,712,  
 1125 doi:10.1029/1999JA000335.  
 1126 Lehtinen, N. G., U. S. Inan, and T. F. Bell (2001), Effects of thunderstorm-  
 1127 driven runaway electrons in the conjugate hemisphere: Purple sprites,  
 1128 ionization enhancements, and  $\gamma$ -rays, *J. Geophys. Res.*, 106(A12),  
 1129 28,841–28,856, doi:10.1029/2000JA000160.  
 1130 Libby, L. M., and H. R. Lukens (1973), Production of radiocarbon in tree  
 1131 rings by lightning bolts, *J. Geophys. Res.*, 78(26), 5902–5903,  
 1132 doi:10.1029/JB078i026p05902.  
 1133 Marshall, T., M. P. McCarthy, and W. D. Rust (1995), Electric field  
 1134 magnitudes and lightning initiation in thunderstorms, *J. Geophys. Res.*,  
 1135 100(D4), 7097–7103, doi:10.1029/95JD00020.  
 1136 McCarthy, M. P., and G. K. Parks (1985), Further observations of X-rays  
 1137 inside thunderstorms, *Geophys. Res. Lett.*, 12(6), 393–396, doi:10.1029/  
 1138 GL012i006p00393.  
 1139 McCarthy, M. P., and G. K. Parks (1992), On the modulation of X-ray  
 1140 fluxes in thunderstorms, *J. Geophys. Res.*, 97(D5), 5857–5864,  
 1141 doi:10.1029/91JD03160.  
 1142 MacDonald, A. D. (1967), *Microwave Breakdown in Gases*, John Wiley,  
 1143 New York.  
 1144 Milikh, G. M., P. N. Guzdar, and A. S. Sharma (2005),  $\gamma$ -ray flashes due to  
 1145 plasma processes in the atmosphere: Role of whistler waves, *J. Geophys.*  
 1146 *Res.*, 110, A02308, doi:10.1029/2004JA010681.  
 Moore, C. B., K. B. Eack, G. D. Aulich, and W. Rison (2001), Energetic  
 radiation associated with lightning stepped leaders, *Geophys. Res. Lett.*,  
 28(11), 2141–2144, doi:10.1029/2001GL013140.  
 Morrow, R. (1985a), Theory of negative corona in oxygen, *Phys. Rev. A*,  
 32, 1799–809.  
 Morrow, R. (1985b), Theory of stepped pulses in negative corona dis-  
 charges, *Phys. Rev. A*, 32, 3821–3824.  
 Moss, G. D., V. P. Pasko, N. Liu, and G. Veronis (2006), Monte Carlo  
 model for analysis of thermal runaway electrons in streamer tips in tran-  
 sient luminous events and streamer zones of lightning leaders, *J. Geo-*  
 1157 *phys. Res.*, 111, A02307, doi:10.1029/2005JA011350.  
 Nemiroff, R. J., J. T. Bonnel, and J. P. Morris (1997), Temporal and spec-  
 1158 tral characteristics of terrestrial  $\gamma$ -flashes, *J. Geophys. Res.*, 102(A5),  
 1159 9659–9665, doi:10.1029/96JA03107.  
 Østgaard, N., T. Gjesteland, J. Stadsnes, P. H. Connell, and B. Carlson  
 (2008), Production altitude and time delays of the terrestrial  $\gamma$ -flashes:  
 Revisiting the Burst and Transient Source Experiment spectra, *J. Geo-*  
 1163 *phys. Res.*, 113, A02307, doi:10.1029/2007JA012618.  
 Rahman, M., V. Corray, N. A. Ahmad, J. Nyberg, V. A. Rakov, and  
 S. Sharma (2008), X rays from 80 cm long sparks in air, *Geophys.*  
 1166 *Res. Lett.*, 35, L06805, doi:10.1029/2007GL032678.  
 Raizer, Y. P., G. M. Milikh, and M. N. Shneider (2010), Streamer - and  
 leader - like processes in the upper atmosphere: Models of red sprites  
 and blue jets, *J. Geophys. Res.*, 115, A00E42, doi:10.1029/  
 2009JA014645.  
 Roussel-Dupré, R., A. V. Gurevich, T. Tunnel, and G. M. Milikh  
 (1994), Kinetic theory of runaway air breakdown, *Phys. Rev. E*, 49(3),  
 1174 2257–2271.  
 Roussel-Dupré, R., and A. V. Gurevich (1996), On runaway breakdown  
 and upward propagating discharges, *J. Geophys. Res.*, 101(A2), 2297–  
 1176 2311, doi:10.1029/95JA03278.  
 Roussel-Dupré, R. A., et al. (2003), Lightning initiation by runaway air  
 1178 breakdown, *Eos. Trans. AGU*, 84(46), Fall Meet. Suppl., Abstract  
 1179 AE31A-01.  
 Roussel-Dupré, R., J. J. Colman, E. Symbalisty, D. Sentman, and V. P. Pasko  
 (2008), Physical processes related to discharges in planetary atmos-  
 1182 pheres, *Space Sci. Rev.*, 137, 51, doi:10.1007/s11214-008-9385-5.  
 Shah, G. N., H. Razdan, G. L. Bhat, and G. M. Ali (1985), Neutron  
 1184 generation in lightning bolts, *Nature*, 313, 773–775.  
 Sharma, A. S., and R. Jayakumar (1988), Runaway electrons during toka-  
 1186 mak startup, *Nucl. Fusion*, 28, 491–506.  
 Shyam, A. N., and T. C. Kaushik (1999), Observation of neutron bursts  
 1188 associated with atmospheric lightning discharge, *J. Geophys. Res.*, 104(A4),  
 1189 6867–6869, doi:10.1029/98JA02683.  
 Smith, D. A., et al. (2002), The Los Alamos Sferic array: A research tool  
 1191 for lightning investigations, *J. Geophys. Res.*, 107(D13), 4183,  
 1192 doi:10.1029/2001JD000502.  
 Smith, D. M., B. J. Hazelton, B. W. Grefenstette, J. R. Dwyer, R. H. Holzworth,  
 and E. H. Lay (2010), Terrestrial gamma ray flashes correlated to storm  
 1195 phase and tropopause height, *J. Geophys. Res.*, 115, A00E49,  
 1196 doi:10.1029/2009JA014853.  
 Smith, D. M., L. I. Lopez, C. P. Lin, and C. P. Barrington-Leigh  
 (2005), Terrestrial  $\gamma$ -ray flashes observed up to 20 MeV, *Science*,  
 1199 307, 1085–1088.  
 Stanley, M. A., et al. (2006), A link between terrestrial  $\gamma$ -ray flashes and  
 1201 intracloud lightning discharges, *Geophys. Res. Lett.*, 33, L06803,  
 1202 doi:10.1029/2005GL025537.  
 Stephanakis, S. J., et al. (1972), Neutron production in exploding wire dis-  
 1204 charges, *Phys. Rev. Lett.*, 29, 568–569.  
 1205  
 Stolzenburg, M., W. D. Rust, B. F. Smull, and T. C. Marshall (1998), Elec-  
 1206 trical structure in thunderstorm convective regions: 1. Mesoscale convec-  
 1207 tive systems, *J. Geophys. Res.*, 103(D12), 14,059–14,078, doi:10.1029/  
 1208 97JD03546.  
 Symbalisty, E. M. D., R. A. Roussel-Dupre, and V. A. Yukhimuk (1998),  
 1210 Finite volume solution of the relativistic Boltzmann equation for electron  
 1211 avalanche studies, *IEEE Trans. Plasma Sci.*, 26, 1575–1582.  
 1212  
 Taranenko, Y. N., and R. Roussel-Dupre (1996), High altitude discharges  
 1213 and  $\gamma$ -ray flashes: A manifestation of runaway air breakdown, *Geophys.*  
 1214 *Res. Lett.*, 23(5), 571–575, doi:10.1029/95GL03502.  
 1215  
 Tsang, K., K. Papadopoulos, A. Drobot, P. Vitello, T. Wallace, and  
 R. Shanny (1991), RF ionization of the lower ionosphere, *Radio*  
 1216 *Sci.*, 26(5), 1345–1360, doi:10.1029/91RS00580.  
 1217  
 Tsuchiya, H., et al. (2009), Observation of an energetic radiation burst from  
 1219 mountain-top thunderclouds, *Phys. Rev. Lett.*, 102, 255003, doi:10.1103/  
 1220 PhysRevLett.102.255003.  
 1221  
 Williams, E. R. (2010), Origin and context of C. T. R. Wilson's ideas on  
 1222 electron runaway in thunderclouds, *J. Geophys. Res.*, 115, A00E50,  
 1223 doi:10.1029/2009JA014581.  
 1224

- 1225 Wilson, C. T. R. (1924), The acceleration of particles in strong electric  
1226 fields such as those of thunderclouds, *Proc. Cambridge Phys. Soc.*, 22,  
1227 534–538.
- 1228 Yukhimuk, V., R. Roussel-Dupre, E. Symbalisty, and Y. Taranenko  
1229 (1998), Optical characteristics of blue jets produced by runaway air  
1230 breakdown, simulation results, *Geophys. Res. Lett.*, 25(17), 3289–3292,  
1231 doi:10.1029/98GL02431.
- Yukhimuk, V., R. A. Roussel-Dupre, and E. M. D. Symbalisty (1999), On 1232  
the temporal evolution of red sprites: Runaway theory versus data, *Geo-* 1233  
*phys. Res. Lett.*, 26(6), 679–682, doi:10.1029/1999GL900073. 1234
- 
- G. Milikh, University of Maryland, College Park, MD 20742, USA. 1235  
(milikh@astro.umd.edu) 1236  
R. Roussel-Dupré, SciTech Solutions, LLC, Santa Fe, NM 87506, USA. 1237  
(bobrdnm@comcast.net) 1238

Article in Proof